Blood sampling

Blood sample was collected with 1:500 dilution of heparin just before euthanizing each animal. Plasma was separated by centrifugation at $1000 \times g$ for 15 min at 4°C and stored at −80°C until analysis. The erythrocyte fraction was washed three times with isotonic NaCl. A stock haemolysate was prepared by the addition of the 2-mercaptoethanol-EDTA stabilizing solution. The concentrated haemolysate was diluted with 2% ethanol immediately before assay.

TBARS in plasma and 8-OH-dG in urine

To assess the level of systemic oxidative stress generated in the process of cardiac remodelling after MI, we measured TBARS in plasma and 8-OH-dG in urine. Plasma TBARS was measured by fluorometric analysis. The plasma was pre-treated with 10% phosphotungstic acid and 1/12 N sulphuric acid. The sample was mixed with a reagent to obtain a final concentration of 7.5% acetic acid, 2 mmol/L EDTA and 0.4% SDS and then reacted with 0.3% thiobarbituric acid (TBA) in a boiling water bath for 45 min. After cooling, the chromogen was extracted in n-butanol/pyridine (15:1, v/v). Fluorescence of the supernatant was measured at excitation and emission wavelengths of 510 and 550 nm, respectively, using a GENios Pro™ (Tecan Group Ltd. Durham, NC). The standard was prepared using 1,1,3,3, -tetraethoxypropane (TEP).

Urine samples were collected in individual metabolic cages (Nalgen, Rochester, NY). After overnight fasting, urine sample was collected from each mouse. Urine 8-OH-dG concentration was determined using a competitive ELISA kit (8-OH-dG check®, Japan, Institute for the Control of Aging, Nagoya, Japan). The value was corrected by urinary creatinine measured with a colorimetric assay kit (Sigma, St. Louis, MO).

TBARS in myocardial tissue

The myocardium was homogenized in 10 volumes of 50 mmol/L sodium phosphate buffer at 4°C for the assay of TBARS in myocardium. The homogenate was centrifuged at $4500 \times g$ for 15 min and the supernatant was used for the biochemical assay of TBARS as in plasma.

Antioxidant enzyme activities in myocardium

To determine the change in capacity of defense during the progression of cardiac remodelling, we measured the levels of antioxidant enzyme activities in the myocardium.

The enzymatic activities of glutathione peroxidase (GPx) and superoxide dismutase (SOD) were measured spectrophotometrically (Tecan Group Ltd., GENios). GPx activity was determined according to the method of Yamamoto and Takahashi [23] by following the oxidation of NADPH in the presence of GR (Oriental Yeast Co., Ltd. Tokyo, Japan), which catalyses the reduction of oxidized glutathione (GSSH) formed by GPx. One enzyme unit is defined as the amount of enzyme that oxidizes 1 μmol of NADPH per minute. SOD activity was examined by the cytochrome c method, in which xanthine and xanthine oxidase (Oriental Yeast Co., Ltd. Tokyo, Japan) were used as a source of superoxide. A unit was defined as the quantity of SOD required for 50% inhibition of the rate of cytochrome c reduction (Wako Pure Chemical Industries, Inc. Osaka, Japan). Protein concentration was determined by the Bradford assay.

Hexanoyl-Lysine adduct (HEL) immunostaining in myocardial tissue

Left ventricular myocardial sections obtained from mice at baseline, day 3 and 28 after MI were immunolabelled by a specific monoclonal anti-HEL antibody (Nikkenn SEIL Corp.). Paraffin-embedded tissue sections (5-μm thick) were deparaffinized with xylene, refixed in Bouin's solution for 20 min, immersed in PBS, incubated with 0.3% H_2O_2 in methanol for 30 min, followed by blocking with M.O.M. mouse IgG blocking reagent. The sections were further incubated with monoclonal anti-HEL antibody in M.O.M. Diluent. After rinsing with 10 mmol/L PBS, they were incubated with biotin-labelled goat anti-rabbit IgG anti-serum (1:100 dilution; DAKO A/S) for 60 min and then with avidin-biotin complex (1:100 dilution; Vectastain ABC kit) for 60 min. After rinsing, the sections were finally incubated with 0.02% 3,3-diaminobenzidine and 0.03% H_2O_2 in deionized water for 6–9 min. As a negative control, sections were incubated with normal rabbit serum instead of anti-HEL antibody.

In vivo *electron spin resonance study*

A spin probe, 3-methoxycarbonyl-2,2,5,5-tetramethylpyrrolidine-1-oxyl (methoxycarbonyl-PROXYL) was synthesized as described previously [24]. For the *in vivo* ESR measurements, 100 mmol/L isotonic methoxycarbonyl-PROXYL was administered (3 μl/g body weight) in mice intravenously. Then ESR spectra were taken at regular intervals using a L-band ESR spectrometer (JEOL Co. Ltd., Akishima, Japan) with a loop-gap resonator (33 mm i.d. and 30 mm in length), as reported previously [25,26]. The power of the 1.1 GHz microwave was 10 mW. The amplitude of the 100-kHz field modulation was 0.063 mT. The signal decay rates, which were used as an index of ROS generation, were determined from the semi-logarithmic plots of signal

intensity vs time after probe injection. Tiron or dimethylthiourea (DMTU) (3 μmol/mouse, dissolved in saline) was administered simultaneously with the probe to confirm the relationship between the signal decay and ROS generation.

Statistical analysis

All data are expressed as mean ± SEM. Between-group comparisons of the means were performed by one-way ANOVA followed by *t*-tests. Bonferroni's correction was done for multiple comparisons of means. A *p*-value less than 0.05 was considered to be statistically significant.

Results

Animal characteristics

The echocardiographic data of surviving mice at days 1, 4, 7, 14 and 28 after MI and control mice are shown in Table I. LV diameters were significantly greater in MI mice at day 4 and thereafter compared to sham-operated control mice. Moreover, MI mice had smaller fractional shortening and anterior wall thickness. There were no alterations in LV diameter and systolic function in sham-operated mice without coronary artery ligation up to day 28 after the operation (data not shown). At day 28, left ventricule LV end-diastolic pressure (LVEDP) was increased in MI (2.6 ± 0.7 vs 14.0 ± 2.3, $p < 0.01$) and LV weight (wt)/body wt (3.12 ± 0.11 vs 3.68 ± 0.17 mg/g, $p < 0.05$), RV wt/body wt (0.88 ± 0.06 vs 1.38 ± 0.11 mg/g, $p < 0.05$), lung wt/body wt (5.36 ± 0.13 vs 7.71 ± 0.80 mg/g, $p < 0.05$) were all increased in MI. The prevalence of pleural effusion was significantly higher in MI (0 vs 50%, $p < 0.01$).

Oxidative byproducts in plasma and urine

Plasma TBARS and urinary 8-OH-dG were significantly elevated at day 1 after MI (Figure 1), and declined to control levels at day 7 and thereafter.

Oxidative markers and antioxidant enzyme activity in myocardial tissue

We measured TBARS (an indicator of lipid peroxidation) and performed immunohistochemical staining of HEL in both infarct and non-infarct myocardial samples. In the infarct area, TBARS increased at day 1 and 7 after MI (Figure 2A). In the non-infarct area, on the contrary, TBARS level was not altered in the early days (days 1, 7 and 14) after MI but was elevated only at day 28.

In agreement with the results of myocardial TBARS, HEL-positive cardiomyocytes were located in the infarct area, whereas there was no staining in the non-infarct area at day 4. (Figure 3). HEL is a novel lipid hydroperoxide modified lysine residue, which is formed by oxidative modification by oxidized ω6 fatty acids such as linoleic acid or arachidonic acid. HEL is a useful biomarker for the initial stage of lipid peroxidation. Although positive staining lasted in the infarct area at day 28, the myocardium was mostly replaced by fibrous tissue and little living myocyte existed. In the non-infarct area, cardiomyocytes were hypertrophied and positively stained by HEL antibody. These suggest that lipid peroxidation starts at an early stage in the infarct area but at late remodelling stage in the non-infarct area. This is consistent with TBARS level in myocardium and indicated increased generation of ROS in the non-infarct area at day 28. The increase of TBARS in the non-infarct area was associated with a significant decline in SOD activity and a tendency of decrease in GPx activity at day 28 (Figure 4).

In vivo *ESR in the heart*

Since TBARS is known to be a non-specific assay to measure lipid peroxidation from biological fluids and tissues and many other substances besides reactive aldehydes react with TBA, we used *in vivo* ESR to determine whether the level of ROS increased in the heart in the remodelling process. Methoxycarbonyl-PROXYL, a stable membrane-permeable nitroxyl radical, is converted into its non-magnetic products, such as its hydroxylamine, immediately after the

Table I. Echocardiographic data.

		Time after MI (days)				
	Control	1	4	7	14	28
n	7	6	6	10	9	8
Heart rate (bpm)	524±22	564±25	552±16	568±23	551±28	589±43
LVEDD (mm)	4.0±0.2	4.5±0.2	5.0±0.2**	5.1±0.2**	5.4±0.1**	5.6±0.2**
LVESD (mm)	2.3±0.2	3.6±0.2**	3.9±0.2**	3.9±0.1**	4.2±0.1**	4.4±0.1**
Fractional shortening (%)	37.6±1.6	21.1±1.6**	22.2±1.6**	23.2±1.6**	20.7±1.0**	21.0±2.7**
Infarct wall thickness (mm)	0.83±0.03	0.60±0.05**	0.61±0.03**	0.44±0.02**	0.44±0.06**	0.30±0.08**
Non-infarct wall thickness (mm)	0.84±0.04	0.80±0.05	1.00±0.02	1.13±0.07*	1.30±0.05**	1.25±0.18**

Control, sham-operated mice; LV, left ventiruclar; EDD, end-diastolic dimension; ESD, end-systolic dimension.
Values are means±SEM. * $p < 0.05$, ** $p < 0.01$ vs controls.

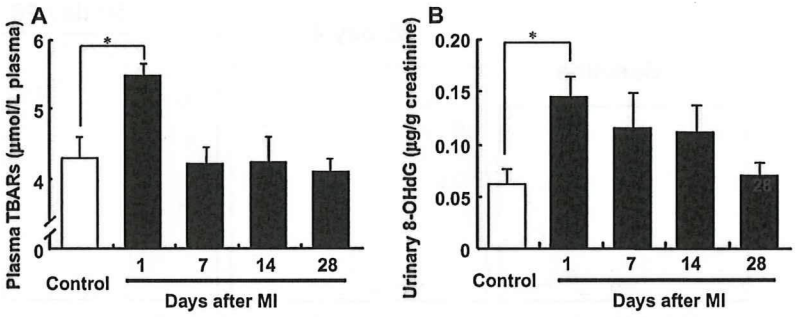

Figure 1. Time-dependent changes of plasma TBARs (A) and urinary 8-OHdG (B) in sham-operated control mice ($n=7$) and mice on day 1 ($n=6$), day 7 ($n=10$), day 14 ($n=9$) and day 28 ($n=8$) after MI. Values are means±SEM. * $p<0.05$, ** $p<0.01$ compared with sham-operated control.

reaction with hydroxy radicals or other reductants. To determine the level of ROS or redox status by *in vivo* ESR measurements, we used methoxycarbonyl-PROXYL as a spin probe which was observed as three sharp lines by ESR spectroscopy (Figure 5A).

We applied signal decay of methoxycarbonyl-PROXYL to *in vivo* ESR to measure ROS generation non-invasively in the failing heart in mice after MI. When the ESR spectrum was measured at the chest level, the signal decay rate was greater in MI mice than sham-operated mice (Figure 5B). The increase of the signal decay observed in MI was suppressed by a simultaneous injection of antioxidants, Tiron or DMTU (Figure 5C and D), indicating the enhancement of free radical reactions at the chest in MI mice. To confirm that the enhancement of signal decay is localized at the chest and does not reflect the increase of systemic free radical generation, the same ESR measurement was repeated at the other parts of the body, head and abdomen from the same animals. ESR signal decay was similar between the two groups when the spectrum was detected at the head and abdominal levels (Figure 5E and F).

Redox alteration during the process of remodelling after MI

Using this *in vivo* ESR technique, we measured free radical production during the time course of remodelling after MI in mice. Radical generation was increased gradually in 4 weeks after MI, which was in parallel to the increase of LVEDD and LVESD and the decrease of EF assessed by echocardiography (Figure 6).

Discussion

In the post-MI myocardium, early remodelling occurs accompanied by infarct expansion, regional dilatation and thinning of the infarct zone and is followed by further deterioration in cardiac performance and increased neurohormonal activation in late remodelling. ROS play an important role in the progression of remodelling in the post-MI myocardium. However, phase-dependent alteration of ROS production in the post-MI myocardium has not been discussed. Moreover, despite a lack of evidence, it is widely misconstrued that an increase of local ROS production is reflected by increases of systemic ROS markers. The present study demonstrates that systemic elevations of ROS markers occur only at the earlier phase after MI. On the contrary, the generation of ROS in non-infarct myocardium is increased from the late phase.

Roles of ROS in the progression of cardiac remodelling

ROS potentially cause cellular damage and dysfunction. Whether the effects of ROS are beneficial or

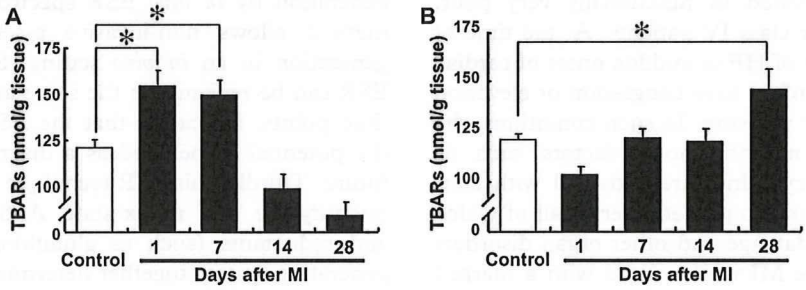

Figure 2. Time-dependent changes of TBARs in infarct (A) and in non-infarct (B) myocardium in sham-operated control ($n=7$) and on day 1 ($n=6$), day 7 ($n=10$), day 14 ($n=9$) and day 28 ($n=8$) after MI. Values are means±SEM. * $p<0.05$ compared with sham-operated control.

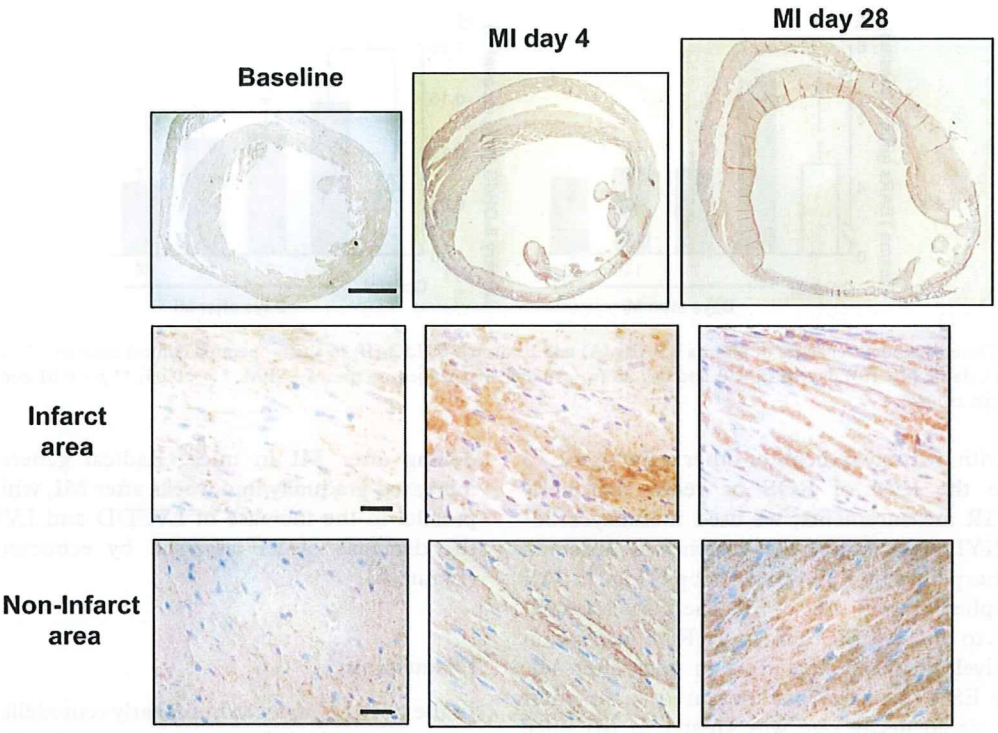

Figure 3. Immunohistochemical detection of HEL moieties in the remodelling process in whole LV, infarct myocardium and non-infarct myocardium, during acute-phase (day 4) and late-phase (day 28) after MI. Scale bar; 1 mm (top) and 10 μm (infarct area and non-infarct area).

harmful depends on the site of action, the source, the amount of ROS generation and the resulting redox balance. Several groups reported that ROS are increased in congestive HF patients [27,28] and accumulating evidence from animal studies revealed that increased ROS play a pivotal role in the pathogenesis and progression of HF [4,9,29–33]. However, whether systemic ROS markers are useful for determining the redox state of the failing heart remains unknown. Li et al. [34] used LC/MS/MS to analyse F_2-isoprostanes in urine from HF patients. They found that only a few peaks were increased, but the most abundant isomer 5-epi-8,12-iso-iP$F_{2\alpha}$-VI was comparable to control subjects. Other clinical studies examined ROS in serum or urine in HF patients by measuring redox markers and reported that ROS are elevated in functionally very poor, NYHA class III or class IV patients. At the time of acute deterioration of HF or sudden onset of cardiac ischemia, patients often have congestion or elevation of LV end diastolic pressure. In such conditions, the immune system, neurohormonal factors such as TNFα and other cytokines are activated with concurrent activation of sympathetic nerve, all of which cause endothelial damage and other organ disorders [35]. In fact, acute MI is associated with a marked increase of inflammatory cells. Previous reports have demonstrated that inflammatory responses and neurohormonal factors cause the generation of oxidative stress not only from the myocardium but also from the vasculature [36–40]. These observations are consistent with our result showing that alteration of systemic ROS markers may not always reflect ROS generation in the myocardium.

Redox status estimated by in vivo ESR

ESR spectroscopy is a useful method to estimate redox status in living animals. In this study, we demonstrated using *in vivo* ESR spectroscopy that increased generation of free radicals in the heart correlated with dilatation of LV and decrease in EF, both of which are indices of the myocardial remodelling process after MI.

There are several advantages to determine ROS generation by *in vivo* ESR spectroscopy. First, the method allows non-invasive assessment of ROS generation in an *in vivo* setting. Secondly, *in vivo* ESR can be repeated in the same animal at different time points, indicating that the ESR technique has the potential to be used as a diagnostic tool in the future. Thirdly, this ESR technique can estimate and quantify the 'net' redox state. Antioxidant enzymes and reductants (such as glutathione) in the ROS generating system together determine the total redox status in biological systems, which may change dynamically and acutely in the heart after MI. Byproducts of free oxygen radicals such as lipid

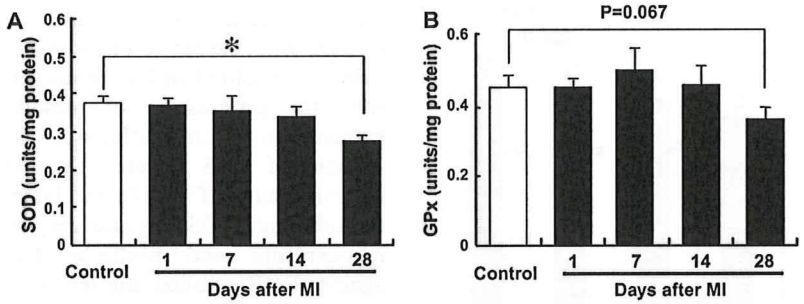

Figure 4. Time-dependent changes of activities of SOD (A) and GPx (B) in non-infarcted myocardium from sham-operated control ($n=7$) and on day 1 ($n=6$), day 7 ($n=10$), day 14 ($n=9$) and day 28 ($n=8$) after MI. Values are means ± SEM. * $p<0.05$ compared with sham-operated control.

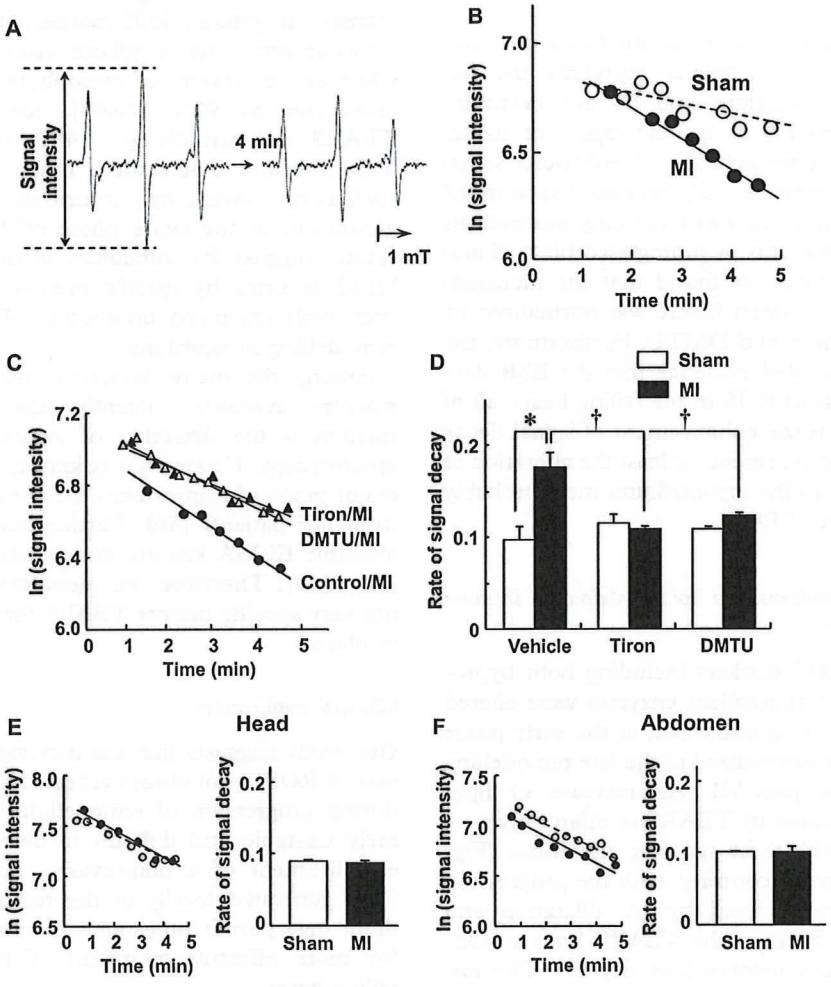

Figure 5. (A) A representative ESR signal of methoxycarbonyl-PROXYL at the chest level of a mouse with myocardial infarction (MI). (B) Semilogarithmic plots of the peak heights of the ESR spectra of methoxycarbonyl-PROXYL after spin probe injection. The signal intensity declined with time, which is defined as the signal decay. (C) The effects of addition of free radical scavengers on the rate of signal decay measured by *in vivo* ESR spectroscopy in individual MI mice. Tiron (a superoxide scavenger) or dimetylthiourea (DMTU; a hydroxyradical scavenger) was injected simultaneously with the injection of methoxycarbonyl-PROXYL. (D) Rates of signal decay measured by *in vivo* ESR in sham and MI groups in the absence and presence of radical scavengers ($n=6$ in each group). *$p<0.01$ vs sham-vehicle group and †$p<0.01$ vs MI-vehicle group. Values are means ± SEM. (E, F) Representative plots of individual mice and rates of *in vivo* ESR signal decay in sham and MI groups ($n=5$ each) measured at the head (E) and abdomen (F).

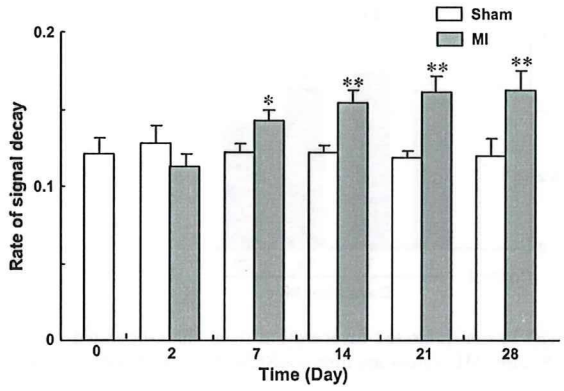

Figure 6. Changes in the rates of signal decay over time measured by *in vivo* ESR spectroscopy in sham and MI mice at days 0, 2, 7, 14 and 28 after operation ($n=7$ in each group). Values are means ±SEM. $*p<0.05$, $**p<.01$ vs sham values for the rate of signal decay.

peroxide, products of protein modifications and DNA damage do not always represent the net capacity of ROS reactions and do not necessary reflect ROS generation in specific organs or tissue. Difficulty in the interpretation of enhanced signal decay has been pointed out, because the nitroxyl radicals are known to react with not only free radicals but also other reductants including ascorbic acid and glutathione. However, we found that the increased ESR signal decay in heart failure was normalized by the addition of Tiron and DMTU. Furthermore, the TBARs study provided evidence that the ESR data reflect the increase of ROS in the failing heart, all of which support that the enhancement of signal decay in late remodelling represents at least the alteration of total redox status in the myocardium, most probably due to an increase of ROS.

Alteration of antioxidants and lipid peroxidation in non-infarct myocardium

We found that ROS markers including both byproducts of ROS and antioxidant enzymes were altered concomitantly in urine and blood at the early phase after MI and were normalized at the late remodelling state at 28 days post-MI. An increase of lipid peroxidation indicated by TBARS in infarct myocardium coincided with these systemic alterations (Figures 1 and 2). On the contrary, with the progression of remodelling represented by LV dilatation and reduced ejection fraction, the TBARS level in non-infarct myocardium increased at day 28. The immunohistochemical analysis by HEL antigen substantiated the finding that ROS was increased in the non-infarct myocardium during late remodelling. It is consistent with our previous findings in a tachycardia-induced canine HF model, in which ROS generation was enhanced in the failing myocardium and correlated with LV end-diastolic pressure and LV ejection fraction [41]. Nevertheless, it remains unknown why oxidative stress was not detectable in urine or in blood in late remodelling after MI, even with the progression of remodelling. A possible explanation is the differences in the source and amount of ROS between the early phase and the chronic phase of HF. In the later phase of post-MI remodelling, ROS increase may occur mainly in the myocardium and multiple defense mechanisms against ROS stabilize the levels in blood and urine. Moreover, ROS is so short-lived that it may not be possible to detect them in urine or blood when the source is localized in a single organ. In contrast, systemic inflammatory responses manifested clinically as leukocytosis and increased cytokines during acute deterioration or sudden ischemia [42–46] may not have enough time to cope with the acute ROS attack and redox change. We suspect that the acute increase in systemic ROS markers after MI is due to systemic activation of inflammatory cells. However, while administration of cyclophosphamide depletes leukocytes by 93% [15,47], the drug inhibited TBARS only partially by ~ 48% (data not shown). This indicates that sources other than leukocytes, such as vasculature, may contribute to systemic ROS generation in the acute phase of MI. All of these results suggest the difficulties of detecting ROS in blood or urine by specific markers in chronic HF, even with enhanced production of ROS from the remodelling myocardium.

Among the many detection techniques of ROS markers available currently, the most sensitive method is the detection of isoprostanes by mass spectroscopy. However, it is known that most of the major peaks of isoprostanes are not elevated in urine from HF patients [30]. Furthermore, commercially available ELISA kits are not as reliable as GC-MS assay [48]. Therefore, we measured a sensitive but not very specific marker TBARS for estimating ROS in plasma.

Clinical implications

Our study suggests that the increased local production of ROS is not always reflected in blood or urine during progression of remodelling. ROS are extremely unstable and difficult to detect directly. The establishment of a non-invasive method to detect ROS generated locally in the remodelling myocardium may permit time- and tissue-targeted therapy for more effective treatment of remodelling and failing heart.

Conclusion

We demonstrated that the generation of ROS in the non-infarct myocardium increases with the progression of cardiac remodelling and this increase is not

reflected by the levels of ROS markers in blood and urine. Clarification of the mechanisms of ROS-mediated remodelling and targeting non-infarct myocardium may lead to novel and effective therapeutic strategies for HF.

Acknowledgements

This study was supported in part by the Uehara memorial foundation and grants from the Ministry of Education (181-00006). A part of this study was conducted in Kyushu University Station for Collaborative Research II.

***Declaration of interest*:** The authors report no conflicts of interest. The authors alone are responsible for the content and writing of the paper.

References

[1] Gheorghiade M, Bonow RO. Chronic heart failure in the United States: a manifestation of coronary artery disease. Circulation 1998;97:282–289.

[2] Cohn JN, Ferrari R, Sharpe N. Cardiac remodeling—concepts and clinical implications: a consensus paper from an international forum on cardiac remodeling. Behalf of an International Forum on Cardiac Remodeling. J Am Coll Cardiol 2000;35:569–582.

[3] Liew CC, Dzau VJ. Molecular genetics and genomics of heart failure. Nat Rev Genet 2004;5:811–825.

[4] Tsutsui H, Ide T, Hayashidani S, Kinugawa S, Suematsu N, Utsumi H, Takeshita A. Effects of ACE inhibition on left ventricular failure and oxidative stress in Dahl salt-sensitive rats. J Cardiovasc Pharmacol 2001;37:725–733.

[5] Ichihara S, Yamada Y, Ichihara G, Kanazawa H, Hashimoto K, Kato Y, Matsushita A, Oikawa S, Yokota M, Iwase M. Attenuation of oxidative stress and cardiac dysfunction by bisoprolol in an animal model of dilated cardiomyopathy. Biochem Biophys Res Commun 2006;350:105–113.

[6] Mollnau H, Oelze M, August M, Wendt M, Daiber A, Schulz E, Baldus S, Kleschyov AL, Materne A, Wenzel P, Hink U, Nickenig G, Fleming I, Munzel T. Mechanisms of increased vascular superoxide production in an experimental model of idiopathic dilated cardiomyopathy. Arterioscler Thromb Vasc Biol 2005;25:2554–2559.

[7] Shite J, Qin F, Mao W, Kawai H, Stevens SY, Liang C. Antioxidant vitamins attenuate oxidative stress and cardiac dysfunction in tachycardia-induced cardiomyopathy. J Am Coll Cardiol 2001;38:1734–1740.

[8] Carlberg I, Mannervik B. Purification and characterization of the flavoenzyme glutathione reductase from rat liver. J Biol Chem 1975;250:5475–5480.

[9] Ide T, Tsutsui H, Kinugawa S, Suematsu N, Hayashidani S, Ichikawa K, Utsumi H, Machida Y, Egashira K, Takeshita A. Direct evidence for increased hydroxyl radicals originating from superoxide in the failing myocardium. Circ Res 2000;86:152–157.

[10] Lang D, Mosfer SI, Shakesby A, Donaldson F, Lewis MJ. Coronary microvascular endothelial cell redox state in left ventricular hypertrophy: the role of angiotensin II. Circ Res 2000;86:463–469.

[11] Kinugawa S, Tsutsui H, Hayashidani S, Ide T, Suematsu N, Satoh S, Utsumi H, Takeshita A. Treatment with dimethylthiourea prevents left ventricular remodeling and failure after experimental myocardial infarction in mice: role of oxidative stress. Circ Res 2000;87:392–398.

[12] Shiomi T, Tsutsui H, Matsusaka H, Murakami K, Hayashidani S, Ikeuchi M, Wen J, Kubota T, Utsumi H, Takeshita A. Overexpression of glutathione peroxidase prevents left ventricular remodeling and failure after myocardial infarction in mice. Circulation 2004;109:544–549.

[13] Matsushima S, Kinugawa S, Ide T, Matsusaka H, Inoue N, Ohta Y, Yokota T, Sunagawa K, Tsutsui H. Overexpression of glutathione peroxidase attenuates myocardial remodeling and preserves diastolic function in diabetic heart. Am J Physiol Heart Circ Physiol 2006;291:H2237–H2245.

[14] Suematsu N, Tsutsui H, Wen J, Kang D, Ikeuchi M, Ide T, Hayashidani S, Shiomi T, Kubota T, Hamasaki N, Takeshita A. Oxidative stress mediates tumor necrosis factor-alpha-induced mitochondrial DNA damage and dysfunction in cardiac myocytes. Circulation 2003;107:1418–1423.

[15] Machida Y, Kubota T, Kawamura N, Funakoshi H, Ide T, Utsumi H, Li YY, Feldman AM, Tsutsui H, Shimokawa H, Takeshita A. Overexpression of tumor necrosis factor-alpha increases production of hydroxyl radical in murine myocardium. Am J Physiol Heart Circ Physiol 2003;284:H449–H455.

[16] Foo RS, Siow RC, Brown MJ, Bennett MR. Heme oxygenase-1 gene transfer inhibits angiotensin II-mediated rat cardiac myocyte apoptosis but not hypertrophy. J Cell Physiol 2006;209:1–7.

[17] Nakagami H, Takemoto M, Liao JK. NADPH oxidase-derived superoxide anion mediates angiotensin II-induced cardiac hypertrophy. J Mol Cell Cardiol 2003;35:851–859.

[18] Siwik DA, Chang DL, Colucci WS. Interleukin-1beta and tumor necrosis factor-alpha decrease collagen synthesis and increase matrix metalloproteinase activity in cardiac fibroblasts *in vitro*. Circ Res 2000;86:1259–1265.

[19] Siwik DA, Pagano PJ, Colucci WS. Oxidative stress regulates collagen synthesis and matrix metalloproteinase activity in cardiac fibroblasts. Am J Physiol Cell Physiol 2001;280:C53–C60.

[20] Matsushima S, Ide T, Yamato M, Matsusaka H, Hattori F, Ikeuchi M, Kubota T, Sunagawa K, Hasegawa Y, Kurihara T, Oikawa S, Kinugawa S, Tsutsui H. Overexpression of mitochondrial peroxiredoxin-3 prevents left ventricular remodeling and failure after myocardial infarction in mice. Circulation 2006;113:1779–1786.

[21] Pimentel DR, Amin JK, Xiao L, Miller T, Viereck J, Oliver-Krasinski J, Baliga R, Wang J, Siwik DA, Singh K, Pagano P, Colucci WS, Sawyer DB. Reactive oxygen species mediate amplitude-dependent hypertrophic and apoptotic responses to mechanical stretch in cardiac myocytes. Circ Res 2001;89:453–460.

[22] Shiomi T, Tsutsui H, Hayashidani S, Suematsu N, Ikeuchi M, Wen J, Ishibashi M, Kubota T, Egashira K, Takeshita A. Pioglitazone, a peroxisome proliferator-activated receptor-gamma agonist, attenuates left ventricular remodeling and failure after experimental myocardial infarction. Circulation 2002;106:3126–3132.

[23] Yamamoto Y, Takahashi K. Glutathione peroxidase isolated from plasma reduces phospholipid hydroperoxides. Arch Biochem Biophys 1993;305:541–545.

[24] Sano H, Matsumoto K, Utsumi H. Synthesis and imaging of blood-brain-barrier permeable nitroxyl-probes for free radical reactions in brain of living mice. Biochem Mol Biol Int 1997;42:641–647.

[25] Han JY, Takeshita K, Utsumi H. Noninvasive detection of hydroxyl radical generation in lung by diesel exhaust particles. Free Radic Biol Med 2001;30:516–525.

[26] Phumala N, Ide T, Utsumi H. Noninvasive evaluation of *in vivo* free radical reactions catalyzed by iron using *in vivo* ESR spectroscopy. Free Radic Biol Med 1999;26:1209–1217.
[27] Belch JJ, Bridges AB, Scott N, Chopra M. Oxygen free radicals and congestive heart failure. Br Heart J 1991;65:245–248.
[28] Dieterich S, Bieligk U, Beulich K, Hasenfuss G, Prestle J. Gene expression of antioxidative enzymes in the human heart: increased expression of catalase in the end-stage failing heart. Circulation 2000;101:33–39.
[29] Ide T, Tsutsui H, Hayashidani S, Kang D, Suematsu N, Nakamura K, Utsumi H, Hamasaki N, Takeshita A. Mitochondrial DNA damage and dysfunction associated with oxidative stress in failing hearts after myocardial infarction. Circ Res 2001;88:529–535.
[30] Cargnoni A, Ceconi C, Bernocchi P, Boraso A, Parrinello G, Curello S, Ferrari R. Reduction of oxidative stress by carvedilol: role in maintenance of ischaemic myocardium viability. Cardiovasc Res 2000;47:556–566.
[31] Guo P, Nishiyama A, Rahman M, Nagai Y, Noma T, Namba T, Ishizawa M, Murakami K, Miyatake A, Kimura S, Mizushige K, Abe Y, Ohmori K, Kohno M. Contribution of reactive oxygen species to the pathogenesis of left ventricular failure in Dahl salt-sensitive hypertensive rats: effects of angiotensin II blockade. J Hypertens 2006;24:1097–1104.
[32] Miwa S, Toyokuni S, Nishina T, Nomoto T, Hiroyasu M, Nishimura K, Komeda M. Spaciotemporal alteration of 8-hydroxy-2′-deoxyguanosine levels in cardiomyocytes after myocardial infarction in rats. Free Radic Res 2002;36:853–858.
[33] Zhang GX, Kimura S, Nishiyama A, Shokoji T, Rahman M, Yao L, Nagai Y, Fujisawa Y, Miyatake A, Abe Y. Cardiac oxidative stress in acute and chronic isoproterenol-infused rats. Cardiovasc Res 2005;65:230–238.
[34] Li H, Lawson JA, Reilly M, Adiyaman M, Hwang SW, Rokach J, FitzGerald GA. Quantitative high performance liquid chromatography/tandem mass spectrometric analysis of the four classes of F(2)-isoprostanes in human urine. Proc Natl Acad Sci USA 1999;96:13381–13386.
[35] Agnoletti L, Curello S, Bachetti T, Malacarne F, Gaia G, Comini L, Volterrani M, Bonetti P, Parrinello G, Cadei M, Grigolato PG, Ferrari R. Serum from patients with severe heart failure downregulates eNOS and is proapoptotic: role of tumor necrosis factor-alpha. Circulation 1999;100:1983–1991.
[36] Kunsch C, Medford RM. Oxidative stress as a regulator of gene expression in the vasculature. Circ Res 1999;85:753–766.
[37] Al-Mehdi AB, Zhao G, Dodia C, Tozawa K, Costa K, Muzykantov V, Ross C, Blecha F, Dinauer M, Fisher AB. Endothelial NADPH oxidase as the source of oxidants in lungs exposed to ischemia or high K+. Circ Res 1998;83:730–737.
[38] Iuchi T, Akaike M, Mitsui T, Ohshima Y, Shintani Y, Azuma H, Matsumoto T. Glucocorticoid excess induces superoxide production in vascular endothelial cells and elicits vascular endothelial dysfunction. Circ Res 2003;92:81–87.
[39] Bertuglia S, Giusti A. Microvascular oxygenation, oxidative stress, NO suppression and superoxide dismutase during postischemic reperfusion. Am J Physiol Heart Circ Physiol 2003;285:H1064–H1071.
[40] Taniyama Y, Griendling KK. Reactive oxygen species in the vasculature: molecular and cellular mechanisms. Hypertension 2003;42:1075–1081.
[41] Aebi H. Catalase *in vitro*. Methods Enzymol 1984;105:121–126.
[42] Nakamura H, Takata S, Umemoto S, Matsuzaki M. Induction of left ventricular remodeling and dysfunction in the recipient heart following donor heart myocardial infarction: new insights into the pathological role of tumor necrosis factor-alpha from a novel heterotopic transplant-coronary ligation model. J Cardiol 2003;41:41–42.
[43] Maury CP. Monitoring the acute phase response: comparison of tumour necrosis factor (cachectin) and C-reactive protein responses in inflammatory and infectious diseases. J Clin Pathol 1989;42:1078–1082.
[44] Guillen I, Blanes M, Gomez-Lechon MJ, Castell JV. Cytokine signaling during myocardial infarction: sequential appearance of IL-1 beta and IL-6. Am J Physiol 1995;269:R229–R235.
[45] Basaran Y, Basaran MM, Babacan KF, Ener B, Okay T, Gok H, Ozdemir M. Serum tumor necrosis factor levels in acute myocardial infarction and unstable angina pectoris. Angiology 1993;44:332–337.
[46] Marx N, Neumann FJ, Ott I, Gawaz M, Koch W, Pinkau T, Schomig A. Induction of cytokine expression in leukocytes in acute myocardial infarction. J Am Coll Cardiol 1997;30:165–170.
[47] Fine PE. Implications of different study designs for the evaluation of acellular pertussis vaccines. Dev Biol Stand 1997;89:123–133.
[48] Pratico D, Lawson JA, Rokach J, FitzGerald GA. The isoprostanes in biology and medicine. Trends Endocrinol Metab 2001;12:243–247.

This paper was first published online on iFirst on 1 December 2008.

Bionic Cardiology: Exploration Into a Wealth of Controllable Body Parts in the Cardiovascular System

Masaru Sugimachi, *Member, IEEE*, and Kenji Sunagawa, *Senior Member, IEEE*

Clilnical Application Review

***Abstract*—Bionic cardiology is the medical science of exploring electronic control of the body, usually via the neural system. Mimicking or modifying biological regulation is a strategy used to combat diseases. Control of ventricular rate during atrial fibrillation by selective vagal stimulation, suppression of ischemia-related ventricular fibrillation by vagal stimulation, and reproduction of neurally commanded heart rate are some examples of bionic treatment for arrhythmia. Implantable radio-frequency-coupled on-demand carotid sinus stimulators succeeded in interrupting or preventing anginal attacks but were replaced later by coronary revascularization. Similar but fixed-intensity carotid sinus stimulators were used for hypertension but were also replaced by drugs. Recently, however, a self-powered implantable device has been reappraised for the treatment of drug-resistant hypertension. Closed-loop spinal cord stimulation has successfully treated severe orthostatic hypotension in a limited number of patients. Vagal nerve stimulation is effective in treating heart failure in animals, and a small-size clinical trial has just started. Simultaneous corrections of multiple hemodynamic abnormalities in an acute decompensated state are accomplished simply by quantifying fundamental cardiovascular parameters and controlling these parameters. Bionic cardiology will continue to promote the development of more sophisticated device-based therapies for otherwise untreatable diseases and will inspire more intricate applications in the twenty-first century.**

***Index Terms*—Biological regulation, feedback control, implantable device, nerve stimulation, system identification.**

I. Introduction

BIONIC cardiology can be defined as medical science in the field of cardiovascular medicine, which explores the electronic control of the body [1], [2]. The term "bionic" derives literally from "bio" (meaning life) and "-onic" (short for electronic). Utilizing the biological amplification mechanism of excitable membranes is an ingenious way to save power and ensure long-term operation of electronic devices. Therefore, the electronic controllers are usually designed to act on specialized tissues such as nerves, skeletal muscles, and myocardium. Since the neural system acts as the control center of the biological regulatory systems, the most efficient way of intervening and controlling the body is to manipulate the neural system.

In the earlier studies of our groups, we defined bionic cardiology in a narrower sense. In developing methods to artificially reconstruct functional defects such as severe orthostatic hypotension (due to loss of pressure stabilization function), we attempted to mimic the biological regulation as precisely as possible [3]–[6] (Fig. 1). To accomplish this, we applied the white-noise approach to unveil the detailed characteristics of complexly integrated biological regulation [4], [7]–[14]. Therefore, by "bionic" cardiology, we meant the reproduction of biological regulation. Although it is not always true (see below), through our efforts in reproducing biological regulation, we began to take full advantage of control engineering in developing artificial controllers. This breakthrough made it possible for us to design feedback closed-loop control rather than open-loop control to achieve therapeutic goals.

Later, we learned that only mimicking biological regulation is not sufficient in treating common diseases. Our body is often affected by common diseases despite the presence of normally functioning biological regulation. In other words, under certain pathophysiological conditions, the normal biological regulation fails to accommodate disease conditions. In some diseases such as heart failure, the biological regulation system may in fact participate in the process of disease evolution and progression. This is best illustrated by the fact that heart failure can be treated with drugs that antagonize biological regulation. Therefore, the strategy to combat these "common" diseases should go beyond the restoration of normal biological regulation. We do not have any model at hand to learn from. In treating common diseases, one has to modify the biological regulation rather than to mimic physiological regulation.

In this paper, we attempt to discuss bionic cardiology in a broader sense, for the reason mentioned above. We also include some earlier studies of open-loop or on-demand control; these examples may serve as a basis for the development of more sophisticated feedback controllers by contemporary control engineering. How we choose short-term therapeutic targets for the feedback control remains a vital question, as the short-term targets are only a proxy for the true endpoint; namely, survival. Nevertheless, the clinical outcome of the predefined target can be appropriately examined only with feedback control.

Manuscript received August 15, 2009. First published October 16, 2009; current version published December 01, 2009. This work was supported in part by the Japan Society for the Promotion of Science under Grant-in-Aid for Scientific Research (S) 18100006 and by the Ministry of Health Labour and Welfare of Japan under Health and Labour Sciences Research Grants H19-nano-ippan-009 and H20-katsudo-shitei-007.

M. Sugimachi is with the Department of Cardiovascular Dynamics, Advanced Medical Engineering Center, National Cardiovascular Center Research Institute, 5658565 Suita, Japan (e-mail: su91mach@ri.ncvc.go.jp).

K. Sunagawa is with the Department of Cardiovascular Medicine, Graduate School of Medical Sciences, Kyushu University, 8128582 Fukuoka, Japan (e-mail: sunagawa@cardiol.med.kyushu-u.ac.jp).

Digital Object Identifier 10.1109/RBME.2009.2034623

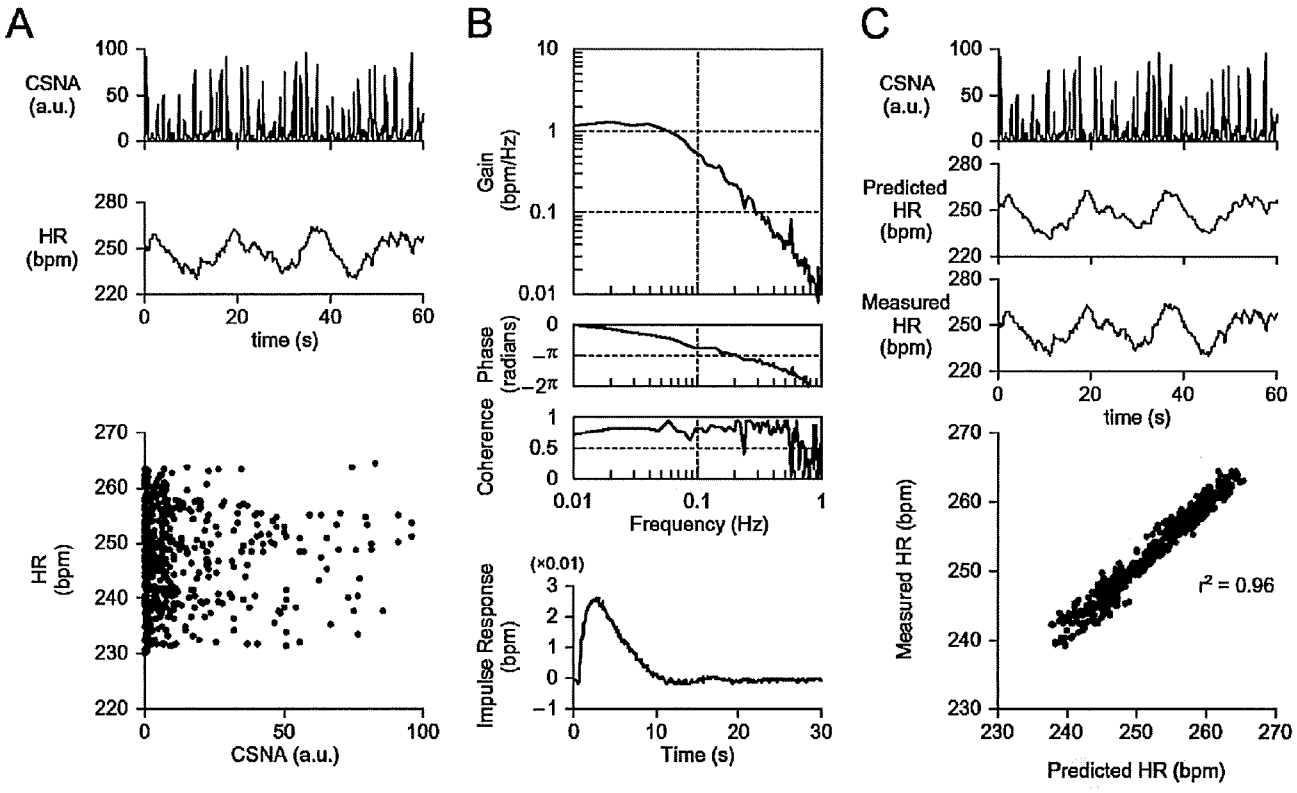

Fig. 1. A representative example of bionic cardiac pacemaker, i.e., neurally regulated pacemaker in a rabbit. (A) Simultaneously measured cardiac sympathetic nerve activity (CSNA) and heart rate (HR). Simple scattergram identified no obvious relationship. (B) Identified linear transfer function and corresponding impulse response to be used for decoding CSNA. (C) Decoded HR (predicted HR) from CSNA correlated well with measured HR. (Reproduced from [1] with permission.)

II. Treatment of Angina Pectoris

Angina pectoris is one form of ischemic cardiac diseases. This may manifest as a chronic stable form for years. Destabilization of atherosclerotic plaques may precipitate acute myocardial infarction resulting in irreversible myocardial loss. In unstable angina, there is an imbalance between oxygen supply and demand and an absolute shortage of coronary blood flow. In the stable form, however, the anginal attack occurs as a result of demand ischemia, usually associated with exertion, emotional stress, and exposure to cold environment. Therefore, a reduction in oxygen demand benefits patients with stable angina. In fact, antianginal drugs such as nitrates and beta-adrenergic blockers are believed to relieve angina by reducing oxygen demand.

A. Carotid Sinus Nerve Stimulation

The treatment of angina by neural intervention was first performed by manual massage of the carotid sinus [15], where the mechanoreceptor exists to feedback-control the autonomic tone. In 1967, Braunwald *et al.* [16] electrically stimulated carotid sinus nerves in two patients with angina, in the same year as Schwartz *et al.* [17] did in patients with hypertension. They used radio-frequency (RF)-coupled neurostimulators. Briefly, the implanted part of the device consisted of two pairs of bipolar platinum electrodes (for bilateral stimulation), coiled stainless steel leads, and a receiver unit. An external battery-driven transmitter delivered RF impulses transcutaneously through an antenna placed just above the receiver.

Carotid sinus nerve stimulation reflexly inhibits sympathetic activity and decreases myocardial oxygen consumption by lowering blood pressure, heart rate, and contractility. Enhanced vagal activity decreases heart rate and may directly decrease contractility [18] in the presence of a high sympathetic tone. Braunwald's group reported that on-demand use of carotid sinus nerve stimulation almost instantly aborted existing anginal attack and prevented the occurrence of new ones [16], [19]. Mason *et al.* [20] compared the effects of nitrates, beta-blockers, and carotid sinus nerve stimulation. Carotid sinus nerve stimulation was considered to reduce preload (as nitrates) and have negative chronotropic and inotropic (as beta-blockers) effects. Vatner *et al.* [19], [21] demonstrated in chronically instrumented conscious dogs that carotid sinus nerve stimulation lowered the resistance of various vascular beds. Of note, coronary vascular resistance also decreased while oxygen demand decreased and was considered to be mediated by sympathetic withdrawal. Solti *et al.* [22], [23] observed that carotid sinus nerve stimulation preferentially increased blood flow in ischemic areas. They attributed this observation to vasodilatation of collateral vessels.

In 1969, Epstein *et al.* [24], [25] treated 17 patients with drug-resistant angina using carotid sinus nerve stimulation. They observed symptomatic relief in 13 of their patients. Angina-interruptive and -prophylactic use of carotid sinus nerve stimulation prolonged exercise duration in 10 and 12, respectively, of the 13 patients. Carotid sinus stimulation had transient adverse effects (pain, cough, paresthesis, and neck tightness sensation; only for around four weeks) that were milder than those

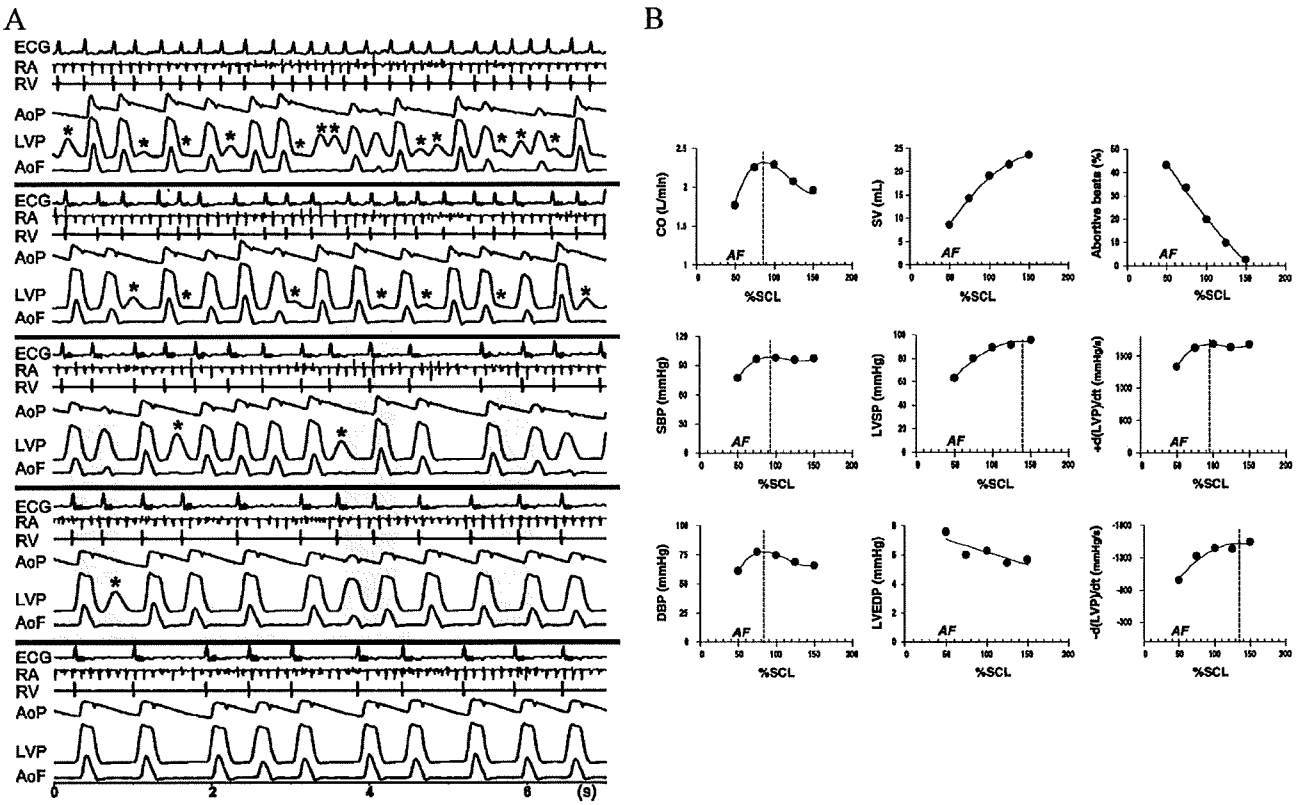

Fig. 2. (A) A representative example of controlling ventricular rate in a dog with atrial fibrillation (AF) by electrical stimulation of vagal nerve at epicardial fat pad innervating atrioventricular node. From top: no control, control to 75%, 100%, 125%, 150% of sinus cycle length (SCL). RA: intracardiac ECG from RA; RV: intracardiac ECG from RV; AoP: aortic pressure; LVP: left ventricular pressure; AoF: aortic flow; (*) abortive beats. (B) Effects of ventricular rate control by fat pad stimulation on hemodynamics in ten dogs. CO: cardiac output; SBP: systolic blood pressure; DBP: diastolic blood pressure; SV: stroke volume; LVSP: left ventricular systolic pressure; LVEDP: left ventricular end-diastolic pressure; $+\mathrm{d(LVP)/dt}$, maximal rate of rise in left ventricular pressure; $-\mathrm{d(LVP)/dt}$, minimal rate of fall in left ventricular pressure. (Reproduced from [33] with permission.)

of vagal stimulation (vomiting, salivation, coughing) [19], [26]. Detailed surgical techniques for carotid sinus stimulation have been described [19], [26]. Carotid sinus nerve stimulation was performed in various institutes worldwide [27]–[29].

Further development of neurostimulator treatment of angina by directly manipulating the autonomic tone is not currently underway, as coronary revascularizations (percutaneous coronary intervention and bypass graft) and potent drugs have become the standard treatments of choice. Recently, however, spinal-cord stimulation used to relieve anginal pain in advanced ischemic heart disease has been reported to also improve some indexes of heart performance [30].

III. Treatment of Arrhythmias

Various forms of arrhythmia have been treated by stimulation of carotid sinus nerves and vagal nerves. Stimulation of carotid sinus nerves involves both the reflex-mediated inhibition of sympathetic nerves and activation of vagal nerves. Heidorn *et al.* [31] showed that massage of the carotid sinus in normal subjects changed the electrocardiogram and concluded that the carotid sinus baroreflex is a physiological phenomenon.

A. Carotid Sinus Nerve Stimulation

Carotid sinus massage was frequently used for bedside diagnosis and treatment of supraventricular tachyarrhythmias [32] in the era when diagnostic tools and antiarrhythmic drugs were limited. Later, Braunwald *et al.* [19] treated patients with supraventricular tachycardia by electrical carotid sinus nerve stimulation, using the same electronic device (Angistat, Medtronic) as used for the treatment of angina (see Section II for details). The authors concluded that electrical stimulation might reduce potential risks such as stroke associated with carotid sinus massage.

B. Vagal Nerve Stimulation

Direct electrical stimulation of the vagal nerve has once been abandoned due to frequent adverse effects. Vagal stimulation, however, has continued to attract the interest of cardiologists for the treatment of refractory arrhythmias including atrial fibrillation and/or life threatening arrhythmias (ventricular fibrillation). Mazgalev *et al.* [33]–[35] (Fig. 2) demonstrated in 18 dogs with simulated atrial fibrillation that electrical stimulation (Itrel II 7424, Medtronic; Photon ICD, St. Jude Medical) of the epicardial fat pad (at the junction of inferior vena cava and left atrium) was able to feedback-control the ventricular rate from 192 to 153 bpm at five weeks. The anatomical selectivity of vagal stimulation in targeting the atrioventricular conduction pathway suggested a minimum risk of adverse effects. In fact, the investigators continued this treatment for five weeks to six months in conscious dogs and reported no noticeable adverse

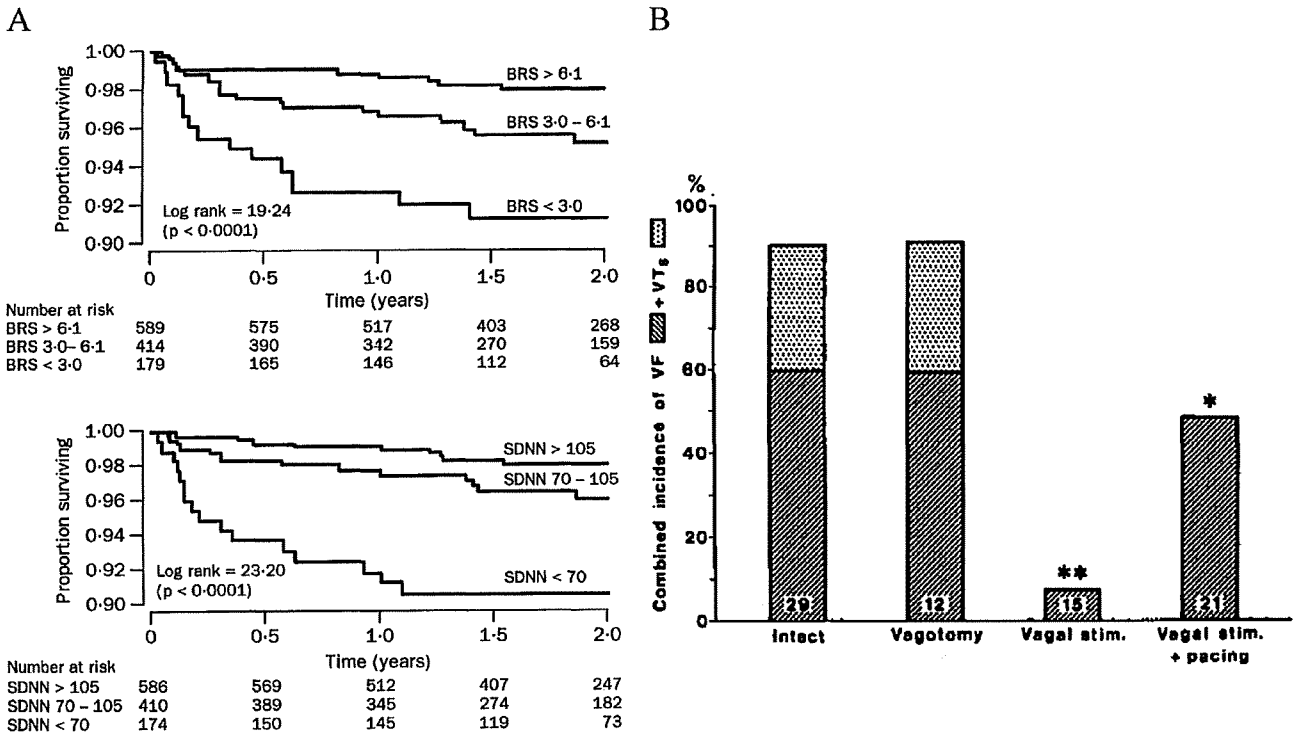

Fig. 3. (A) Survival (free from cardiac death or aborted cardiac arrest) in patients after myocardial infarction, plotted by baroreflex sensitivity (BRS) or by heart rate variability (SDNN). (B) Effect of efferent vagal stimulation (with vagotomy) started soon before reperfusion on incidence of Vf and sustained ventricular tachycardia (VTs) in cats with coronary occlusion and reperfusion. (*) $p < 0.005$ versus intact and $p < 0.05$ versus vagotomy. (**) $p < 0.001$ versus intact and vagotomy. (Reproduced from [43] (A) and [44] (B) with permission.)

effects [34]. They also proposed that the preservation of normal ventricular conduction pathway outweighed the hemodynamic effect of the loss of atrial contraction, as shown by comparing the rate control by fat pad stimulation and atrioventricular nodal ablation with right ventricular pacing [35], [36]. This finding is consistent with the equivalent outcomes of rate and rhythm control in recent large clinical trials [37]. Even in a patient with severe heart failure, short-term endocardial stimulation of fat pad has succeeded in rate control and eventual restoration from a decompensated state [38].

Vagal stimulation enhanced with choline esterase inhibitor, beta-adrenergic blocker, and/or calcium blocker has once been used to induce temporary asystole for surgical procedures [39]. Atrial vagal denervation (ablation) was attempted to prevent atrial fibrillation associated with excessive vagal activity but with limited success [40].

Using a clinically relevant disease model (healed anterior myocardial infarction superimposed with acute ischemia during exercise), Cerati and Schwartz [41] found that the residual vagal activity during ischemia protects against fatal ventricular fibrillation. The same group succeeded in quantifying the background vagal activity with baroreflex sensitivity index (increase in RR interval for a given increase in blood pressure). Higher pre- (>20 versus < 14 ms/mmHg) and postinfarction (>15 versus < 9 ms/mmHg) baroreflex sensitivity predicted resistance to ventricular fibrillation in dogs (risk of ventricular fibrillation, 35% versus 85%, and 20% versus 91%, respectively, both $p < 0.001$) [42]. In large clinical trials (ATRAMI), higher baroreflex sensitivity predicted better outcomes [43] [Fig. 3(A)]. The same group showed that electrical vagal stimulation even beginning just before reperfusion (i.e., at the end of ischemia) was protective against ventricular fibrillation during reperfusion [44] [Fig. 3(B)]. Ando *et al.* [45] proposed that vagal stimulation exerts anti-arrhythmogenic effects by preserving the functional connexin in intercellular junctions thereby maintaining synchronicity between myocardial cells.

C. *Neurally Regulated Artificial Pacemaker*

Artificial pacemakers are the ultimate solution for bradyarrhythmias. Although the pacemakers guarantee the rate of cardiac contractions, they are unable to reproduce native physiological rate regulation. Ikeda *et al.* [4] developed a pacemaker that reproduced physiological regulation of heart rate. They succeeded to decode the heart rate response from sympathetic nerve activity as the central message and found the decoding rule by a white-noise approach [4], [8], [9]. The root mean square error of heart rate control relative to the native heart rate was 1.4 to 6.6 bmp or $1.2 \pm 0.7\%$ of mean heart rate [4] (Fig. 1). The success of deciphering the central autonomic neural messages opens up new applications of regulating artificial organs directly by measuring the autonomic nervous activity. It allows the artificial organs to operate as if they are an integral part of the native system.

IV. Treatment of Hypertension

Hypertension is universally the most prevalent risk factor that aggravates atherosclerotic diseases. Despite numerous studies

over many years, the true cause of elevated blood pressure remains unsolved in most patients. Since lowering blood pressure delays the atherosclerotic process, numerous antihypertensive drugs have been developed and used clinically. Electronic treatment of hypertension was first developed for patients with severe drug-resistant hypertension at the time when fewer drugs were available. In recent years, however, the development of advanced neurostimulators as well as the recognition of a large population with drug-resistant hypertension have promoted the reappraisal of this device treatment.

A. *Classical Neurostimulation*

Hypertension has been treated electronically, almost exclusively by electrical stimulation of the carotid sinus nerve, which reflexly induces withdrawal of sympathetic nerve activity. Griffith *et al.* [46] investigated the effect of unilateral carotid sinus nerve stimulation in normal and renal hypertensive dogs. Except in hypertensive dogs with contralateral carotid sinus nerve sectioned, the hypotensive effect of carotid sinus nerve stimulation gradually decreased in 50 min. This attenuation may be partly due to the counteracting effect of remaining intact baroreflex components.

The first implantable carotid sinus neurostimulator was developed in the University of Minnesota by two surgeons [47]. This device delivered fixed-intensity stimulation synchronous to R wave to bilateral carotid sinus nerves. When evaluated in dogs, blood pressure was dramatically decreased in hypertensive dogs compared to normal dogs (systolic effect of 40–50 mm Hg versus 20 mmHg). Motivated by the study of direct carotid sinus nerve stimulation in man [48], Schwartz *et al.* [17] applied three types of baropacers (primary-celled, rechargeable, RF-coupled) to unilateral carotid sinus nerve in patients. In eight of 11 patients followed for five months to 2.5 years, the depressive effects persisted (systolic effect: 30–100 mmHg; diastolic effect: 24–80 mmHg). Agishi *et al.* [49] used mercury column as an on-off switch to automatically control pressure in dogs. Brest *et al.* [50] (eight patients) and Solti *et al.* [51] (one patient) described their experience of using a commercially available RF-coupled device (Barostat, Medtronic) for stimulating bilateral carotid sinus nerve. Using an externally worn transmitter, RF-coupled device allowed long-term treatment and external control of pulse amplitude and width. Electrical stimulation-induced hypotension was accompanied by bradycardia, a lower rate of pressure rise, lower cardiac index, and a decrease in vascular resistance relative to the level expected from significant hypotension.

Despite these earlier reports, device treatment of hypertension has almost disappeared until recently, due to the development of various classes of useful antihypertensive drugs. Moreover, in spite of reports of sustained hypotensive effect of carotid sinus nerve stimulation for over two years [50], arguments against the role of arterial baroreflex in chronic blood pressure regulation have gained widespread support. These arguments were based on the observation that blood pressure almost normalizes a few days after experimental sinoaortic denervation. This finding seemingly supports the notion of complete resetting of baroreflex and the role of the renin-angiotensin-aldosterone system in maintaining long-term blood pressure.

B. *Role of Baroreflex Revisited in the Pathogenesis of Hypertension*

Recently, using a carotid sinus nerve stimulation with neurostimulator (CVRx), Lohmeier *et al.* [52]–[57] showed that seven days of carotid sinus nerve stimulation induced sustained decrease in blood pressure associated with decrease in plasma norepinephrine but without increase in renin activity, suggesting a powerful role of baroreflex in chronic arterial pressure regulation [Fig. 4(A)]. The authors suggested that decreased renal sympathetic activity inhibits the increase in renin secretion during hypotension and enhances renal sodium secretion. The hypotensive effect did not persist in angiotensin-induced hypertension due to increased angiotensin level and when sympathetic tone and renin level were already suppressed before carotid sinus nerve stimulation [53] but did persist in obesity-induced hypertension [56]. Carotid sinus nerve stimulation decreased blood pressure to a greater extent than complete beta- and alpha1-adrenergic blockade, suggesting the pathophysiological relevance of postsynaptic alpha2-adrenergic mechanism [57]. Based on these results, the authors concluded that baroreflex is involved in chronic pressure regulation. Even though the resetting of baroreceptors cannot be denied, central resetting of baroreflex seems very small.

Another line of evidence also supports the role of baroreflex in chronic pressure regulation. Thrasher [58]–[64] has shown that chronic baroreceptor unloading (baroreceptor denervation except one carotid sinus, and ligation of common carotid artery of the remaining innervated carotid sinus) produces rather different pressor response than sinoaortic denervation. Chronic baroreceptor unloading maintained pressor response for at least seven days [58] [Fig. 4(B)], and although pressor response was reduced at five weeks, the magnitude was significantly greater than that of sinoaortic denervation [62] (decreased response may be due to increased sinus pressure by back pressure). He attributed the difference between chronic baroreceptor unloading and sinoaortic denervation to central adaptation in sinoaortic denervation. Reports by Munch *et al.* [65] on incomplete (56%) chronic resetting also supported a role of baroreflex in chronic pressure regulation. Taken together, there is no question that baroreflex plays a significant role in chronic blood pressure regulation. Hence a new model of carotid sinus neurostimulator (Rheos, CVRx), which is an external RF signal controllable, self-powered implantable device with long-life battery, would be a powerful clinical tool in controlling drug-resistant hypertension.

Unlike fixed-intensity carotid sinus nerve stimulation, development of sophisticated real-time feedback closed-loop neurostimulator requires control engineering. In an old article by Warner [66], the author failed to attenuate externally imposed cyclic pressure disturbances by a simple increase in baroreceptor gain. He correctly attributed this to the delay in pressure regulation. On the contrary, Kubota *et al.* [3] have shown that properly identified baroreceptor transduction in terms of transfer function reproduces similar level of pressure stability as native baroreflex.

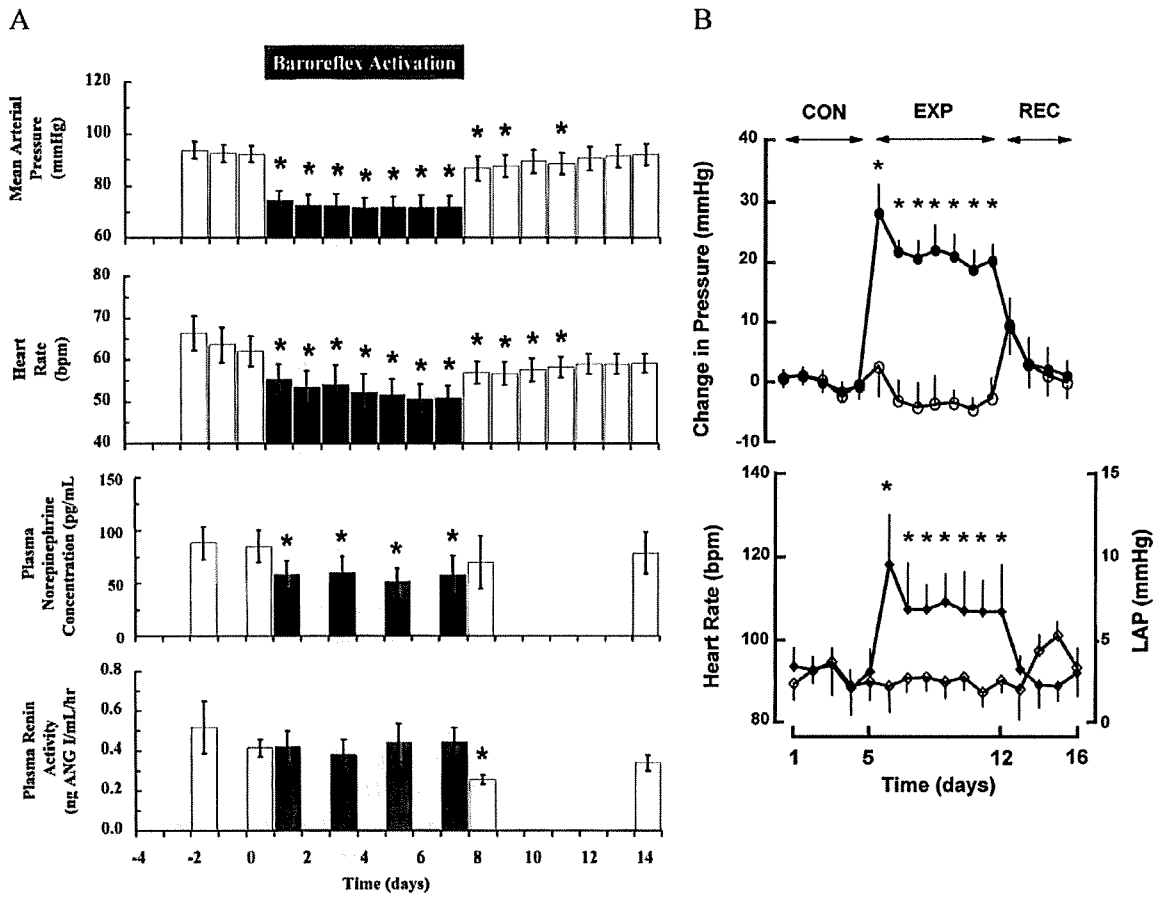

Fig. 4. (A) Effect of continuous baroreflex activation (bilateral carotid sinus stimulation) on mean arterial pressure, heart rate, plasma norepinephrine concentration, and plasma renin activity for seven days in six dogs. Due to decreased sympathetic activity, hypotension did not increase renin or decrease sodium excretion. (*) $p < 0.05$. (B) Chronic baroreceptor unloading (barodenervation and ligation of common carotid artery of the one remaining innervated carotid sinus) continuously increased blood pressure (closed circle) and heart rate (closed diamond) for seven days in dogs ($n = 5 \sim 6$). Open circle: carotid sinus pressure; open diamond: left atrial pressure (LAP). CON: control; EXP: baroreceptor unloading; REC: recovery; (*) $p < 0.05$. (Reproduced from [52] (A) and [58] (B) with permission.)

C. *Electroacupuncture*

Electrical acupuncture stimulation may be used to decrease blood pressure and decrease sympathetic nerve activity [67]–[70] [Fig. 5(A)]. Acupuncture stimulation changes the static properties of the central baroreflex controller in a direction of decreasing maximal sympathetic activity [67] [Fig. 5(A)] without changing the dynamic properties [68]. Kawada *et al.* [69] succeeded in developing a feedback depressor system by acupuncture in cats [Fig. 5(B)].

V. Treatment of Hypotension

Unlike hypertension, control of pressure against hypotension has been outside the scope of bionic cardiology. However, transient hypotension during, for example, postural change is one of the best targets for bionic cardiology for the following reasons. Severe orthostatic hypotension occurs as a result of damage to any of the components of the arterial baroreflex, including baroreceptors (neck surgery, radiation), vasomotor centers (Shy–Drager syndrome), and efferent pathways (spinal-cord injury). Hypotension is usually profound and requires prompt restoration with much shorter delay than is possible with any available drug to avoid syncope. Chronic pressor treatments should be avoided, as continuous hypertension increases the risk for atherosclerosis. For the above reasons, pharmacological treatments, either continued or on-demand, are obviously inappropriate. As patients may lose consciousness with sudden hypotension, fully automatic feedback control of pressure should be developed.

A. *Open-Loop Characterization of Baroreflex System*

To accomplish feedback pressure control, Sato *et al.* [10] and Kawada *et al.* [11] analyzed static open-loop characteristics of the two subsystems of the baroreflex: controller (discharging sympathetic nerve traffic in response to sensed pressure) and plant (changing pressure according to sympathetic nerve traffic). The actual operating pressure is determined by the intersection (i.e., equilibrium) between the two functional curves of subsystems. Sato *et al.* [12] and Ikeda *et al.* [13] analyzed the open-loop transfer functions over a wide frequency range. They demonstrated that the transfer function of the plant approximates a second order low-pass filter. In contrast, they demonstrated that the transfer function of the controller possesses derivative characteristic. By analyzing

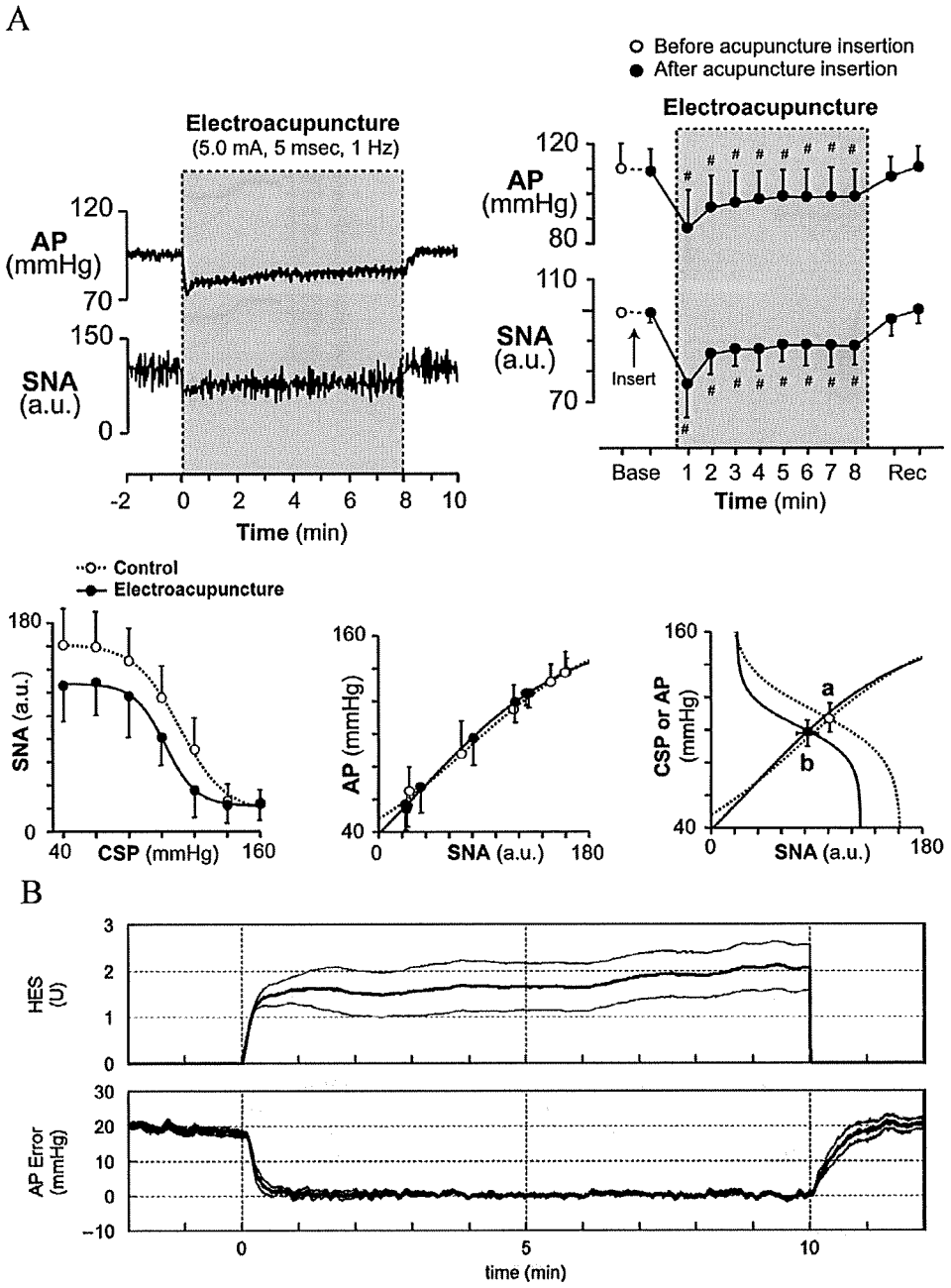

Fig. 5. (A) Electroacupuncture at Zusanli acupoint decreases arterial pressure (AP) and cardiac sympathetic nerve activity (SNA) for 8 min in six rabbits with intact baroreflex (top). Left: a representative example; right: pooled data (#) $p < 0.05$ versus baseline after acupuncture insertion. Hypotensive and sympathoinhibitory effect were due to the changes in controller (bottom left) but not plant (bottom center) of baroreflex. CSP: carotid sinus pressure. (B) Feedback control of AP by acupuncture-like hind-limb electrical stimulation (HES) in eight cats. Changes in HES is translated into changes in stimulus intensity (if HES > 1) and into changes in stimulus frequency (if HES < 1). (Reproduced from [67] (A) and [69] (B) with permission.)

these transfer functions, Ikeda *et al.* [13] have shown that the normal biological baroreflex is optimal to achieve quick and stable closed-loop responses.

B. Bionic Feedback Pressure Regulation

With the basic data at hand [14], Sato *et al.* [5], [6] designed a bionic baroreflex system by mimicking the functional biological baroreflex. The controller was designed so that the transfer function of the cascade of the controller and the biological plant (for stimulation of sympathetic celiac ganglion) matches that of the total-loop baroreflex. Therefore, the transfer function of the desired controller was obtained from the ratio of the transfer function of total-loop baroreflex to that of the plant. In ten rats depleted of functional baroreflex [6], the application of bionic baroreflex during a head-up tilt significantly ($p < 0.05$) attenuated blood pressure drop from 34 ± 6 to 21 ± 5 mmHg at 2 s, and from 52 ± 5 to 15 ± 6 mmHg at 10 s. The residual pressure drop was not different from that observed in rats with intact baroreflex [Fig. 6(A)].

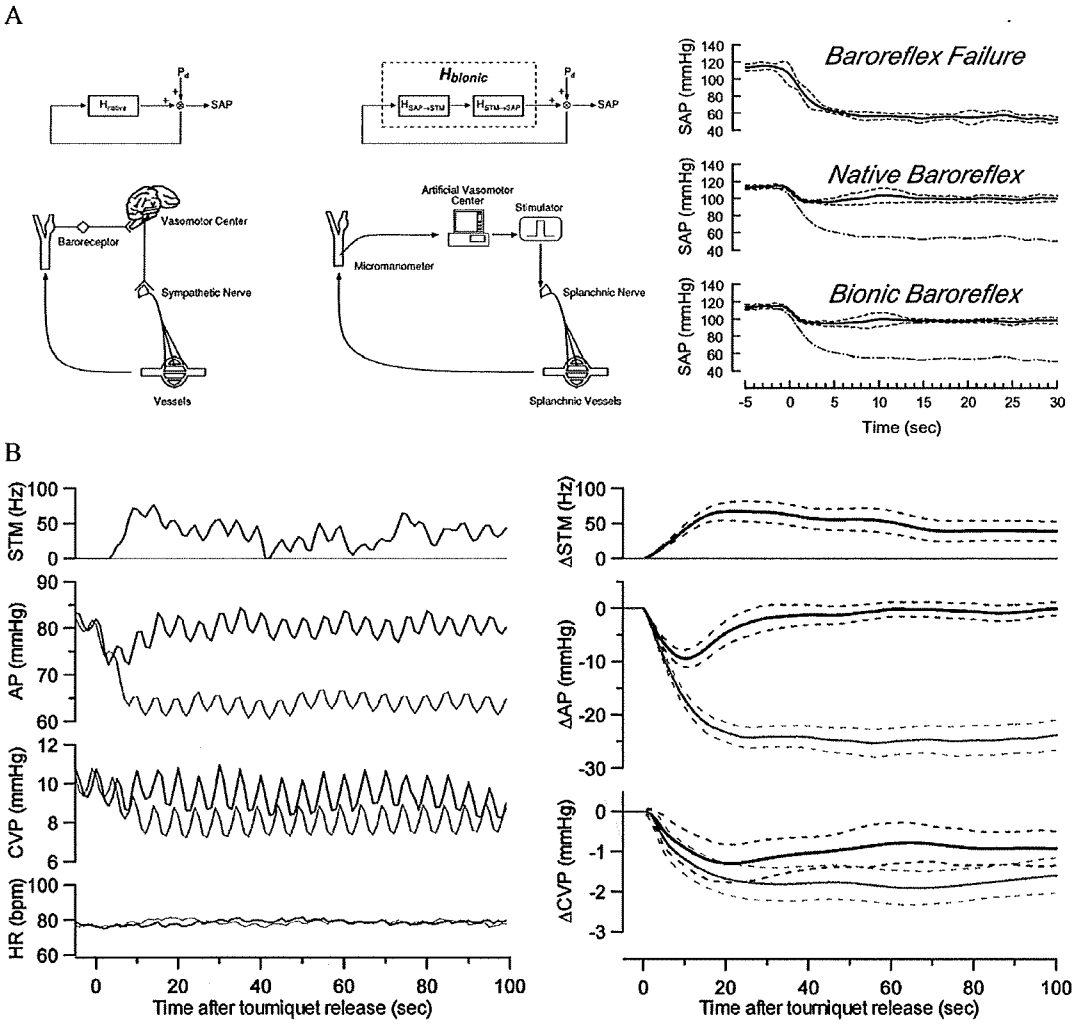

Fig. 6. (A) Functional and anatomical diagram of native baroreflex (left) and bionic baroreflex (center). Pd: pressure perturbation; SAP: systemic arterial pressure; H_{native}: open-loop transfer function of native baroreflex; H_{bionic}: open-loop transfer function of total bionic baroreflex; $H_{SAP \rightarrow STM}$: transfer function of designed bionic baroreflex controller; $H_{STM \rightarrow SAP}$: transfer function of native baroreflex plant. Changes in SAP in baroreflex failure, native baroreflex, and bionic baroreflex after head-up tilt (right). Dash-dot lines: average response in baroreflex failure. (B) Hypotension after tourniquet release was prevented by bionic baroreflex system using epidural spinal cord stimulation. Left: a representative patient; right: pooled data from 21 patients. STM: stimulation frequency; AP: arterial pressure; CVP: central venous pressure, HR: heart rate. (Reproduced from [5], [6] (A) and [72] (B) with permission.)

Yanagiya *et al.* [71] constructed a bionic baroreflex system using spinal cord stimulation via an epidural electrode catheter in six cats. They [71] designed the controller to provide quick and stable control only, rather than to mimic the biological controller. The system ameliorated a drop in pressure from 37 ± 5 to 21 ± 2 mmHg at 5 s and 59 ± 11 to 8 ± 4 mmHg at 30 s ($p < 0.05$). Epidural spinal-cord stimulation was further clinically applied by Yamasaki *et al.* [72] during surgery in a selected group of patients ($n = 12$) undergoing knee surgery. Pressure drop after tourniquet deflation was suppressed significantly ($p < 0.05$) from 17 ± 3 to 9 ± 2 mmHg at 10 s and 25 ± 2 to 1 ± 2 mmHg at 50 s [Fig. 6(B)]. Various inputs other than direct sympathetic stimulation may change blood pressure [67]–[70], [73]–[75]. Even noninvasive transcutaneous electrical stimulation [76] was developed for suppressing hypotension in patients with spinal-cord injury. In 12 patients, bionic feedback control restored the pressure drop by 50% in 35 ± 12 s and by 90% in 60 ± 18 s.

VI. Treatment of Heart Failure

A. Neurohormonal Activation Plays Major Roles in the Pathogenesis of Heart Failure

Heart failure is a complex syndrome that can result from any kind of cardiac diseases at their advanced stage. Mortality with this syndrome is considerably high even with the development of state-of-art treatments including artificial hearts, regenerative medicine, and cardiac transplantation. Recently, implantable device-based treatment of heart failure has attracted physicians' interest because of its enormous impact on survival. Available devices include implantable cardiac defibrillator to terminate fatal arrhythmia and cardiac resynchronization treatment device to improve the synchronicity of left ventricular contraction and hence cardiac performance. Device for bionic treatment of heart failure is now under aggressive development to complement the roles of these devices.

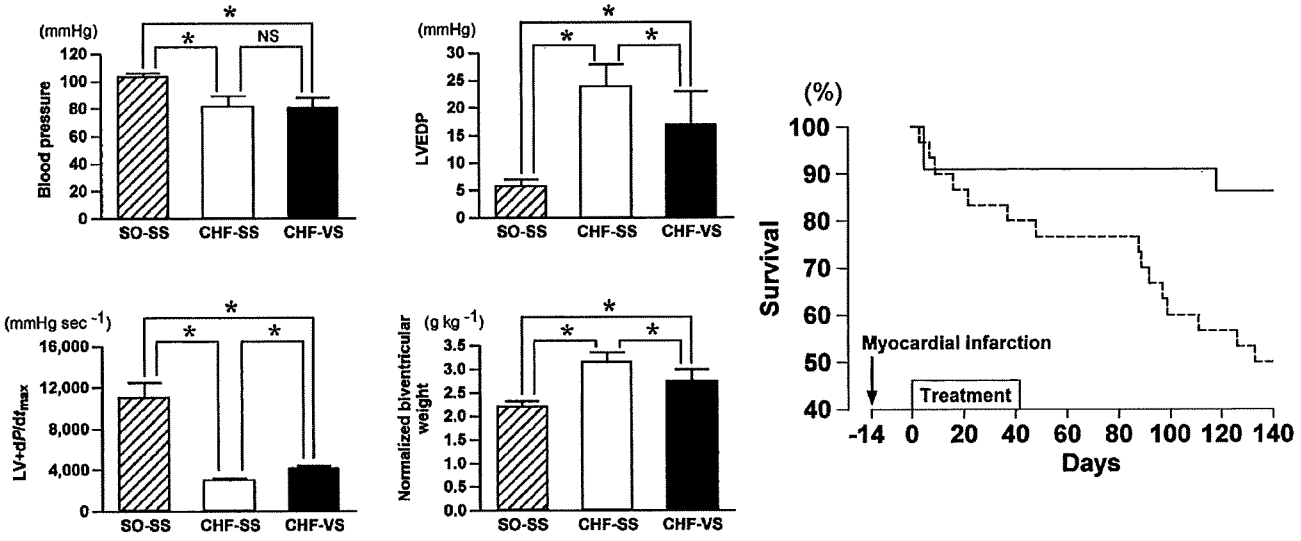

Fig. 7. Forty-two-day right vagal stimulation attenuated increased LVEDP, decreased maximal rate of left ventricular pressure rise (LV $+dP/dt_{max}$), increased normalized biventricular weight (left). SO-SS: sham-stimulated rats without failure (n = 9); CHF-SS: sham-stimulated rats with heart failure (n = 13); CHF-VS: vagal-stimulated rats with heart failure (n = 11); (*) $p < 0.05$. Survival for 140 days of rats with (solid line, n = 22) or without (dashed line, n = 30) 42-day vagal stimulation (right). (Reproduced from [78] with permission.)

Although the primary cause of heart failure is decreased pump function, the adjunct neurohumoral activation is certainly a major aggravating factor for disease progression and risk of death. Clinical trials on drugs for heart failure have revealed repeatedly that suppression of neurohumoral factors rather than increasing cardiac contractility improves survival. Pharmacological activation of vagal tone (such as low-dose scopolamine) [77] has been evaluated, but the effects on long-term survival have not been shown. With this background, bionic device therapy counteracting activated neurohumoral factors has been developed.

B. *Vagal Nerve Stimulation in Animal Studies*

Li *et al.* [78] first demonstrated that direct electrical stimulation of right vagal nerve (started after healing of extensive myocardial infarction) was effective in delaying the progression of heart failure and drastically improving survival in rats with heart failure. The intensity of vagal stimulation was low (decreasing heart rate by approximately 10%) enough to avoid adverse effects. They showed that vagal stimulation (control, n = 13; vagal stimulation, n = 11) significantly decreased left ventricular filling pressure from 24 ± 4 to 17 ± 6 mmHg, increased left ventricular $+dp/dt_{max}$ from 2987 $\pm$ 192 to 4152 ± 37 mmHg/s and decreased biventricular weight from 3.1 ± 0.2 to 2.8 ± 0.3 g/kg body weight, although the size of infarction was unchanged. Vagal nerve stimulation markedly improved survival from 50% to 82% ($p < 0.01$) at 140 days (Fig. 7). The same group also showed that vagal stimulation suppressed arrhythmias [79] and decreased both vasopressin secretion and salt ingestion [80]. The latter indicates the possible contribution of central modification induced by afferent nerve stimulation. Heart rate decreased progressively in six weeks. Vagal nerve stimulation protected the heart against acute ischemia, as well as reduced norepinephrine [81] and myoglobin [82] (an index of myocardial injury) release. These effects were attributed to its bradycardiac effect. Uemura *et al.* [83] investigated the effect of vagal nerve stimulation (−15 to 240 min) on matrix metalloproteinase (MMP) activity in a rabbit model of ischemia (60 min)-reperfusion (180 min) injury. Vagal stimulation increased the expression of tissue inhibitor of MMP-1 (TIMP-1) in cardiomyocytes and reduced active MMP-9. These molecular mechanisms of vagal stimulation might help prevent cardiac remodeling.

Some of the beneficial effects of vagal stimulation in heart failure may involve anti-inflammatory pathways. A large body of evidence [84]–[89] indicates that both afferent and efferent vagal nerves form anti-inflammatory pathways. The afferent vagal nerve senses local inflammation and transmits the information to the brain to suppress excessive inflammatory response in other areas in which inflammation may be elicited by the diffusion of various cytokines. In addition to recruiting the hypothalamic-pituitary-adrenal axis to release corticoids, the efferent vagal nerve is activated for faster anti-inflammatory response. The efferent activity stimulates nicotinic receptors on macrophages [84], and nicotinic alpha7 unit is essential for this regulation [86]. Activation of nicotinic receptors inhibits the release of pro-inflammatory cytokines such as TNF-alpha, IL-5, and IL-18 but does not inhibit the anti-inflammatory cytokine IL-10 [84]. Efferent vagal nerve stimulation is shown to decrease liver NF-kappa B, reduce plasma TNF-alpha, and revert hypotension in hemorrhagic shock (besides septic shock) through nicotinic receptors [89]. These findings indicate the involvement of inflammatory response in life-threatening cardiovascular disease such as hemorrhagic shock and heart failure.

C. *Vagal Nerve Stimulation in Patients With Heart Failure*

Recently, an implantable chronic vagal neurostimulator has entered clinical trial [90]. In this small-sized trial, the stimu-

lator (Cardiofit, BioControl) was implanted in 32 patients with heart failure (NYHA II to III, ejection fraction $\leq$ 35%). The right vagal nerve was stimulated intermittently (4 mA, 21% on). Heart rate decreased from 82 to 76 bpm; quality-of-life score (Minnesota Living with Heart Failure Questionnaire) improved from 48 to 32; 6-min walk increased from 410 to 471 m; and left ventricular ejection fraction increased from 23% to 27% in six months. The impact of vagal stimulation on the hard endpoint in these patients remains to be seen.

D. Carotid Sinus Nerve Stimulation in Heart Failure

Zucker *et al.* [91] examined if carotid sinus nerve stimulation (CVRx) improves the survival of dogs with pacing-induced (250 bpm) heart failure. They continued tachypacing until the endpoint (death or moribund state) was reached. Although the progression of heart failure (indicated by left ventricular end-diastolic pressure, left ventricular $+dp/dt_{max}$, mean arterial pressure, heart rate, ejection fraction) was similar between dogs with and without carotid sinus nerve stimulation, increases in norepinephrine and angiotensin II were delayed in dogs with carotid sinus nerve stimulation. Dogs with carotid sinus nerve stimulation survived longer. How this observation translates to the clinical impact of carotid sinus nerve stimulation in patients with heart failure remains to be investigated.

VII. Autopilot Treatment of Acute Decompensated Heart Failure

Although neurohumoral suppression is the mainstay of long-term treatment for heart failure, a different strategy is required when the hemodynamics are acutely exacerbated. In order to save the lives of such patients, vital hemodynamic variables including blood pressure, cardiac output, and left atrial pressure have to be maintained within physiological ranges. Abnormality in each of these variables should be corrected promptly. The management of hemodynamic decompensation requires complex control of infusions of multiple potent drugs. The advent of automated feedback control of multiple drug infusions would have a major impact on clinical medicine. Such closed-loop feedback treatment involves control engineering and electronic controllers. This is also an important area of bionic cardiology.

A. Development of Integrative Cardiovascular Model

Various modalities of feedback control of hemodynamic variables using drug infusion have been attempted [92], [93], including those that control two variables. These attempts were only partially successful due to the complex interaction between variables. Results of these investigations prompted Uemura *et al.* [94], [97], [98] to take a different approach for hemodynamic control. They first established methods to break down each hemodynamic variable into fundamental physiological properties of the cardiovascular system. This was achieved by modeling the total cardiovascular system as the interaction of three different components: left heart pump, right heart pump, and total (systemic and pulmonary) vasculature [94], [96]. The model is an extension of Guyton's cardiovascular model [95] but differs from Guyton's model in several aspects: a third axis is incorporated to explicitly express left atrial pressure; the left and right heart pump functions are defined independently; and blood redistribution between systemic and pulmonary vasculature is expressed on the same venous return surface [Fig. 8(A)]. Using this model, Uemura *et al.* [94], [97] succeeded in delineating fundamental determinants of hemodynamics (left heart pump function, right heart pump function, systemic vascular resistance, and total stressed blood volume) from clinically measurable variables (blood pressure, cardiac output, left atrial pressure, and right atrial pressure).

B. Bionic Treatment of Decompensated Heart Failure

Based on their new model, Uemura *et al.* [98] designed a bionic controller that can simultaneously normalize blood pressure, cardiac output, and left atrial pressure accurately, quickly, and stably [Fig. 8(B)]. Their success is based on the effective decoupling of the complex interaction between variables, thereby allowing them to design three independent feedback control loops: left heart pump function controlled by an inotropic agent (dobutamine), systemic vascular resistance controlled by a vasodilator (sodium nitroprusside), and total stressed blood volume controlled by a volume expander and/or a diuretic (dextran solution, furosemide). Using the controller in 12 anesthetized dogs with severely decompensated heart failure restored the pump function, vascular resistance, and blood volume to normal levels in 30 min. As a result, blood pressure was controlled within 4.4 ± 2.6 mmHg, cardiac output within 5.4 ± 2.4 ml/min/Kg, and left atrial pressure within 0.8 ± 0.6 mmHg for another 30 min. The average amounts of drug use was dobutamine 4.7 ± 2.6 μg/min/kg, nitroprusside 4.2 ± 1.8 μg/min/kg, dextran infusion 2.4 ± 1.9 mL/kg, and furosemide 10 mg in one dog and 20 mg in another dog [Fig. 8(C)]. Even using the classical proportional-integral control for dobutamine and nitroprusside infusions and the "if-then" rule control for dextran/furosemide, control of multiple hemodynamic variables was possible and of good quality.

C. Beyond Hemodynamic Stabilization

Uemura *et al.* [99] attempted to further elaborate the treatment of decompensated heart failure beyond hemodynamic stabilization. They added myocardial oxygen consumption as an additional target for electronic control. The heart is an organ that consumes a large amount of oxygen and is highly vulnerable to oxygen shortage. Hayashida *et al.* [100] have shown in conscious dogs that the heart optimizes its metabolic efficiency during exercise as well as at rest. Theoretically, the optimal heart rate minimizes oxygen consumption for a given blood pressure, cardiac output, and left atrial pressure [101]. Uemura *et al.* [99] demonstrated in conscious dogs with acute decompensated heart failure that the automated electronic system of hemodynamic management allowed them to pharmacologically lower heart rate and myocardial oxygen consumption without compromising hemodynamics. The model-based approach to simultaneous optimization of multiple variables would help improve the outcome of patients with hemodynamic decompensation.

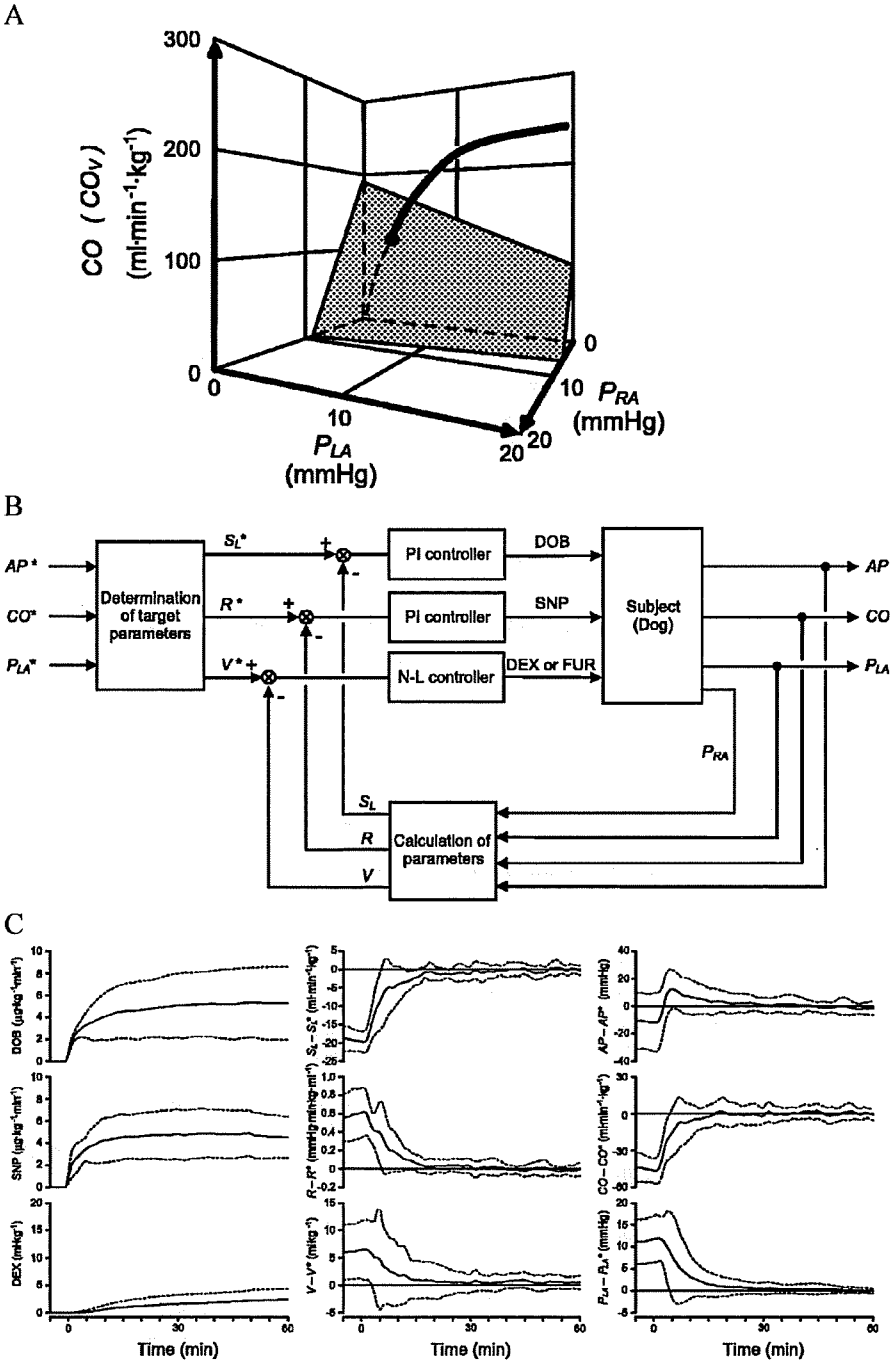

Fig. 8. (A) Extended Guyton's model of the total cardiovascular system. A third axis explicitly expresses left atrial pressure (P_{LA}), a cardiac output curve expresses left and right heart pump function independently, and a venous return surface expresses blood distribution in vasculatures. P_{RA}: right atrial pressure; CO: cardiac output; CO_V: venous return (= cardiac output). (B) Block diagram of an autopilot system for simultaneous control of systemic arterial pressure (AP), CO, and P_{LA}. Parameters with (*) indicate target values. From target variables, target values of left heart pump function (S_L), stressed blood volume (V), and systemic vascular resistance (R) are determined. S_L, V, and R of subjects are calculated from measured AP, CO, P_{LA}, and P_{RA}. Proportional-integral (PI) controllers adjust infusion rate of dobutamine (DOB) and sodium nitroprusside (SNP) to minimize the error in S_L and R, respectively. If-then rules adjust infusion of 10% dextran 40 (DEX) or injection of furosemide (FUR) to minimize the error in V. (C) Automatic correction of acute decompensated heart failure. Errors in cardiovascular properties (middle panels) (S_L, R, V) rapidly approached to zero, resulting in cardiovascular variables (right panels) (AP, CO, P_{LA}) approaching respective target. Left panels indicate infusion rate of DOB, SNP, and infused volume of DEX. (Reproduced from [98] with permission.)

VIII. Future of Bionic Medicine

We foresee a promising future for bionic medicine. It appears, however, that various factors may significantly influence the development and promotion of bionic cardiology. The first is the technology to interface native regulatory systems with bionic systems. The latest technology has made it possible to physically interface electronic devices with cardiac tissues (pacemaker, ICD). Neural interface, however, leaves much room for

improvement in terms of selectivity, stability, and durability. Sophistication of physical as well as logical neural interface will no doubt facilitate intricate body control. An advanced interface that allows stimulation at lower electrical power by minimizing current leakage and fully utilizing native excitation function will reduce adverse effects. Appropriate methods for the selective measurement and/or stimulation of subgroup of nerve fibers are necessary to match the spatial resolution indicated by the physiological/medical requirements. Autonomic function may be the first controllable function in the clinical setting compared to sensory or motor functions where intricate neural interface for higher spatial and temporal resolution is mandatory.

The second is the development of implantable long-term sensors. This factor would appear to be one of the basic needs, but has been relatively ignored until recently. For years, measurements have been limited to electrical signals. No durable sensors for mechanical or chemical variables are available. Once implanted, it is necessary to keep its accuracy even in blood for a considerably long term without repeated recalibrations. Therefore, the requirements of such sensors include long-term durability, stability, anticoagulation nature, and no need for recalibration.

The third is technology to support communication mechanisms in the body. Since the operation of bionic system is based on a closed feedback mechanism, various feedback loop components including sensors, controllers, actuators and plant have to communicate mutually. In the body, the neurohormonal mechanisms support this communication. In the bionic system, however, if some of these components are physically distant from each other, artificial communication mechanisms are needed for closed loop operation. We await the development of such an artificial communication mechanism in the body. The communication should simultaneous satisfy the short delay time (for real-time operation and closed-loop feedback), the sufficient bandwidth (depending on the application), the avoidance from interference from other communications and noises (guaranteeing secure feedback operation), and the mission-critical security (for medical need).

The fourth is the mechanism to support the power of bionic devices. This has been a significant problem, and will remain a target for research. The battery life should be long enough to be clinically meaningful. The size is preferable as small as possible. This is because the size of power supplies often determines that of the implantable devices. The third and fourth technology, if realized and combined, may obviate the use of leads, the most fragile part of implantable devices.

The fifth is the development of integrative science for biological system. To design elaborate feedback regulation of the cardiovascular system, in-depth knowledge of biological regulation is essential. Moreover, as already discussed in the Introduction, we have to go beyond the restoration of biological regulation to combat common diseases. Biological regulation has to be translated into and expressed in the "language" of control engineering. The expression should include dynamic, multiple-input, interactive, nonlinear, and feedback natures of the total system concerned. Besides these, we have to develop a model incorporating the effect of modifying biological regulation on the progression of common diseases. The development of such a model definitely requires biological research. Investigations of integrative biological regulation mandate the knowledge of both biology and engineering. It is our hope that many biomedical engineers will participate in the exploration into the development of bionic medicine.

The last factor is medical needs. Recent interest in device-based therapy will uncover the potential of bionic medicine in meeting the unmet needs. Of various cardiovascular diseases presented in this paper, the need for the appropriate treatment of chronic heart failure is most seriously unmet. Device-based therapy including bionic medicine is expected to complement existing treatment modalities to provide therapeutic benefits that cannot be achieved by drugs alone, especially for the increasing patients of chronic heart failure.

In conclusion, bionic medicine is the science to explore the wealth of controllable body parts. Bionic cardiology has a long history, through which we have accumulated much experience, generated knowledge on biological regulation, and identified unmet needs. These unique features together put us in a strong position to promote the development of more sophisticated device-based therapy for otherwise untreatable diseases. Bionic medicine will inspire more intricate applications in the twenty-first century.

REFERENCES

[1] T. Kawada and M. Sugimachi, "Artificial neural interfaces for bionic cardiovascular treatments," *J. Artif. Organs*, vol. 12, no. 1, pp. 17–22, Mar. 2009.

[2] M. Sugimachi and K. Sunagawa, "Bionic cardiovascular medicine. Functional replacement of native cardiovascular regulation and the correction of its abnormality," *IEEE Eng. Med. Biol. Mag.*, vol. 24, pp. 24–31, Jul.-Aug. 2005.

[3] T. Kubota, H. Chishaki, T. Yoshida, K. Sunagawa, A. Takeshita, and Y. Nose, "How to encode arterial pressure into carotid sinus nerve to invoke natural baroreflex," *Amer. J. Physiol.*, vol. 263, no. 1, pp. H307–H313, Jul. 1992.

[4] Y. Ikeda, M. Sugimachi, T. Yamasaki, O. Kawaguchi, T. Shishido, T. Kawada, J. Alexander Jr., and K. Sunagawa, "Explorations into development of a neurally regulated cardiac pacemaker," *Amer. J. Physiol.*, vol. 269, no. 6, pp. H2141–H2146, Dec. 1995.

[5] T. Sato, T. Kawada, T. Shishido, M. Sugimachi, J. Alexander Jr., and K. Sunagawa, "Novel therapeutic strategy against central baroreflex failure: A bionic baroreflex system," *Circulation*, vol. 100, no. 3, pp. 299–304, Jul. 1999.

[6] T. Sato, T. Kawada, M. Sugimachi, and K. Sunagawa, "Bionic technology revitalizes native baroreflex function in rats with baroreflex failure," *Circulation*, vol. 106, no. 6, pp. 730–734, Aug. 2002.

[7] M. Sugimachi, T. Imaizumi, K. Sunagawa, Y. Hirooka, K. Todaka, A. Takeshita, and M. Nakamura, "A new method to identify dynamic transduction properties of aortic baroreceptors," *Amer. J. Physiol.*, vol. 258, no. 3, pp. H887–H895, Mar. 1990.

[8] T. Kawada, Y. Ikeda, M. Sugimachi, T. Shishido, O. Kawaguchi, T. Yamazaki, J. Alexander Jr., and K. Sunagawa, "Bidirectional augmentation of heart rate regulation by autonomic nervous system in rabbits," *Amer. J. Physiol.*, vol. 271, no. 1, pp. H288–H295, Jul. 1996.

[9] T. Kawada, M. Sugimachi, T. Shishido, H. Miyano, Y. Ikeda, R. Yoshimura, T. Sato, H. Takaki, J. Alexander Jr., and K. Sunagawa, "Dynamic vagosympathetic interaction augments heart rate response irrespective of stimulation patterns," *Amer. J. Physiol.*, vol. 272, no. 5, pp. H2180–H2187, May 1997.

[10] T. Sato, T. Kawada, M. Inagaki, T. Shishido, H. Takaki, M. Sugimachi, and K. Sunagawa, "New analytic framework for understanding sympathetic baroreflex control of arterial pressure," *Amer. J. Physiol.*, vol. 276, no. 6, pp. H2251–H2261, Jun. 1999.

[11] T. Kawada, T. Shishido, M. Inagaki, C. Zheng, Y. Yanagiya, K. Uemura, M. Sugimachi, and K. Sunagawa, "Estimation of baroreflex gain using a baroreflex equilibrium diagram," *Jpn. J. Physiol.*, vol. 52, no. 1, pp. 21–29, Feb. 2002.